European Journal of Medicinal Chemistry 150 (2018) 698–718

Contents lists available at ScienceDirect

European Journal of Medicinal Chemistry

journal homepage: http://www.elsevier.com/locate/ejmech

Research paper

Antimalarial agents against both sexual and asexual parasites stages: structure-activity relationships and biological studies of the Malaria Box compound 1-[5-(4-bromo-2-chlorophenyl) furan-2-yl]-*N*-[(piperidin-4-yl)methyl]methanamine (MMV019918) and analogues

Alessandra Vallone [a, b, d, 1], Sarah D'Alessandro [b, d, e, 1], Simone Brogi [a, b, d], Margherita Brindisi [a, b, d], Giulia Chemi [a, b, d], Gloria Alfano [a, b, d], Stefania Lamponi [a, b], Soon Goo Lee [f], Joseph M. Jez [f], Karin J.M. Koolen [g], Koen J. Dechering [g], Simona Saponara [c], Fabio Fusi [c], Beatrice Gorelli [c], Donatella Taramelli [b, d, h], Silvia Parapini [b, d, h], Reto Caldelari [i], Giuseppe Campiani [a, b, d, **], Sandra Gemma [a, b, d, *], Stefania Butini [a, b, d]

[a] Department of Biotechnology, Chemistry and Pharmacy, Dipartimento di Eccellenza 2018-2022, University of Siena, Via Aldo Moro 2, 53100, Siena, Italy
[b] European Research Centre for Drug Discovery and Development (NatSynDrugs), University of Siena, Via Aldo Moro 2, 53100, Siena, Italy
[c] Department of Life Sciences, University of Siena, Via Aldo Moro 2, 53100, Siena, Italy
[d] Centro Interuniversitario di Ricerche sulla Malaria (CIRM), University of Perugia, Perugia, Italy
[e] Dipartimento di Scienze Biomediche, Chirurgiche e Odontoiatriche, Università di Milano, Via Pascal 36, 20133, Milan, Italy
[f] Department of Biology, Washington University in St. Louis, St. Louis, MO, 63130, United States
[g] TropIQ Health Sciences, Transistorweg 5-C02, 6534 AT, Nijmegen, The Netherlands
[h] Dipartimento di Scienze Farmacologiche e Biomolecolari, Università di Milano, Via Pascal 36, 20133, Milan, Italy
[i] Institute of Cell Biology, University of Bern, Baltzerstrasse 4, 3012, Bern, Switzerland

ARTICLE INFO

Article history:
Received 24 July 2017
Received in revised form
6 March 2018
Accepted 8 March 2018
Available online 10 March 2018

Keywords:
Malaria
Gametocytes
Plasmodium falciparum
Inhibition
Structure-activity relationships

ABSTRACT

Therapies addressing multiple stages of *Plasmodium falciparum* life cycle are highly desirable for implementing malaria elimination strategies. MMV019918 (**1**, 1-[5-(4-bromo-2-chlorophenyl)furan-2-yl]-*N*-[(piperidin-4-yl)methyl]methanamine) was selected from the MMV Malaria Box for its dual activity against both asexual stages and gametocytes. In-depth structure-activity relationship studies and cytotoxicity evaluation led to the selection of **25** for further biological investigation. The potential transmission blocking activity of **25** versus *P. falciparum* was confirmed through the standard membrane-feeding assay. Both **1** and **25** significantly prolonged atrioventricular conduction time in Langendorff-isolated rat hearts, and showed inhibitory activity of Ba^{2+} current through $Ca_v1.2$ channels. An *in silico* target-fishing study suggested the enzyme phosphoethanolamine methyltransferase (*Pf*PMT) as a potential target. However, compound activity against *Pf*PMT did not track with the antiplasmodial activity, suggesting the latter activity relies on a different molecular target. Nevertheless, **25** showed interesting activity against *Pf*PMT, which could be an important starting point for the identification of more potent inhibitors active against both sexual and asexual stages of the parasite.

© 2018 Elsevier Masson SAS. All rights reserved.

1. Introduction

Despite recent advances in the field of antimalarial treatment, malaria is still responsible for a high number of infections and related deaths in tropical and sub-tropical regions [1]. The

* Corresponding author. Department of Biotechnology, Chemistry and Pharmacy, Siena, Italy
** Corresponding author. Department of Biotechnology, Chemistry and Pharmacy, Siena, Italy.
E-mail addresses: campiani@unisi.it (G. Campiani), gemma@unisi.it (S. Gemma).
[1] These authors equally contributed to the present work.

http://dx.doi.org/10.1016/j.ejmech.2018.03.024
0223-5234/© 2018 Elsevier Masson SAS. All rights reserved.

antimalarial agenda has currently shifted from malaria control to eradication/elimination strategies. To reach this ambitious goal and to complement appropriate vector-control measures, such as larvicidal compounds and insecticide-treated bed nets, prioritization of new approaches, targeting the transmission stages of *Plasmodium falciparum* life cycle (i.e. the gametocytes) is necessary [2]. Development of dual acting drugs active against asexual intra-erythrocytic parasites, responsible for the clinical symptoms of malaria, and gametocytes, the sexual forms of the parasite responsible for malaria transmission, is a challenging goal but necessary for the implementation of the above-mentioned strategies.

High-throughput screening (HTS) assays have been successfully applied to *P. falciparum* asexual stages for the discovery of novel hits endowed with innovative modes of action [3–14]. Moreover, such approaches have been adapted for the discovery of compounds active as gametocytocidal agents [15–24]. Screening campaigns using these assays allowed a better analysis and characterization of the anti-gametocyte properties of known antimalarials and for the discovery of potential hit compounds useful for the development of transmission-blocking therapies [25]. The implementation of novel methodologies of phenotypic screening for gametocytocidal compounds was recently boosted by the non-profit foundation Medicine for Malaria Venture (MMV), which produced and delivered a collection of 400 commercial compounds divided into 200 drug-like and 200 probe-like structures, i.e., the "Open Access Malaria Box" [26]. The structures present in the Malarial Box were selected using results from phenotypic screening of large compound collections against *P. falciparum* [3,27,28]. These phenotypic screens identified nearly 20,000 compounds that were active against *P. falciparum* 3D7 and endowed with reasonable toxicity. Selection criteria for compounds included in the Malaria Box were commercial availability, maximization of the structural diversity, and potency.

A cell-based assay with *P. falciparum* gametocytes expressing a potent luciferase and a lactate dehydrogenase (LDH)-based gametocyte assay were used to screen known antimalarial compounds and those of the MMV Malaria Box [23,25,26]. From this initial study, compound MMV019918 (**1**, Chart 1) [26] demonstrated dual activity against *P. falciparum* asexual and sexual stages with $IC_{50} < 1000$ nM; an *in vitro* $IC_{50} < 1000$ nM against late stages *Plasmodium* gametocytes consistently found in different published assays (and also in the structurally related compound *N*-[(5-(3-chloro-4-fluorophenyl)furan-2-yl)methyl]-*N*,*N*′-dimethylpropane-1,3-diamine (MMV020505, **2**)) [25]; activity on both male and female NF54 gametes; and properties favorable for drug development, including a low molecular weight and a scaffold suitable for optimization of efficacy. Starting from compound **1** and combining synthetic and biological efforts, we investigated the structure-activity relationships (SAR) of this class of compounds with the aim of understanding the general structural features important for the observed activity. Our goal was also to investigate and possibly improve the toxicity profile of the prepared analogues since the selectivity index (SI) of **1** was rather low based on the available information, and a certain degree of *h*ERG activity (83% of inhibition at 50 μM) was also known for this compound [25].

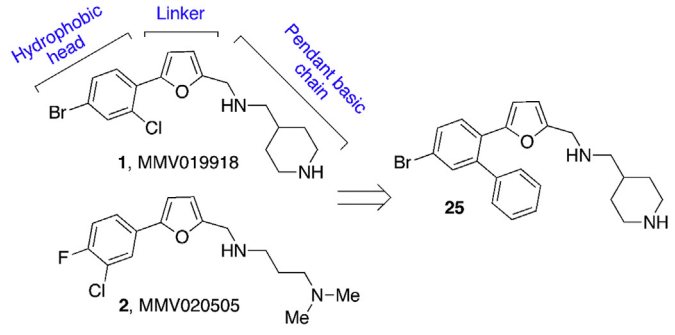

Chart 1. Structure of the reference compounds **1**,**2** and of the analogue **25**.

The SAR investigation of **1** was based on the possibility of disconnecting its scaffold into three modules: a hydrophobic head, a heterocyclic linker, and a pendant basic chain (Chart 1). We introduced different substituents, at the hydrophobic head to explore the role of the two halogen substituents, replaced the central linker with different heterocyclic scaffolds, and replaced the cyclic piperidine moiety with linear lateral chains. Compound **25**, showing comparable potency with respect to **1**, characterized by the presence of and extra aromatic ring at the hydrophobic head and endowed with reasonable TC_{50}, was then selected for further biological studies.

2. Results and discussion

2.1. Chemistry

We identified a synthetic strategy for the preparation of the hit compound **1** that was also suitable for the preparation of a broad series of analogues bearing different substitution patterns at the phenyl ring.

As displayed in Scheme 1, the first step to the synthesis of **1** and analogues **8**–**12** was a Suzuki-Miyaura coupling between aryliodides **3a-f** and the organoboronic acid **4** [29] to afford aldehydes **5a-f**. In the case of derivatives **5a,c,d**, this palladium-catalyzed cross coupling reaction turned out to be exquisitely regioselective for the formation of reaction products arising from attack at the most reactive iodine with respect to other halides. In the subsequent steps of the synthesis, aldehydes **5a-f** and **6** (in turn obtained from **5f** by deprotection) were reacted with the primary amine **7** and the resulting imine intermediates were reduced using sodium cyanoborohydride. Final removal of the piperidine protecting group upon exposure to acidic conditions led to the final compounds **1** and **8**–**12**.

Amine **7** was prepared starting from *N*-Boc-piperidone **13**, which was subjected to a Wittig reaction using (methoxymethyl) triphenylphosphonium chloride and sodium bis(trimethylsilyl) amide [30] resulting in an intermediate vinylmethyl ether that was hydrolyzed using cerium chloride and sodium iodide [31] to afford aldehyde **14**. This latter compound was reduced to the corresponding alcohol, which was converted into methanesulfonate and reacted with sodium azide to furnish **15**. The final catalytic hydrogenation, using palladium on carbon, led to the formation of the desired piperidinyl-methanamine **7** in satisfactory yield.

Because of the unavailability of the starting aryliodides, a second set of compounds, modified at the hydrophobic head, was synthesized using a different chemical route (Scheme 2). For the synthesis of aldehydes **5a and 18b-e**, the Meerwein arylation protocol [32], consisting in a copper-catalyzed arylation of furan derivatives with arenediazonium salts, was conveniently used. According to this procedure, anilines **16a-e** were converted into the corresponding diazonium salts, and these latter intermediates were coupled in situ with furan-carboxaldehyde **17**. Intermediates **5a and 18b** were also submitted to a Suzuki coupling to afford the biphenyl derivatives **19a,b**, respectively. Aldehydes **5a,18b-e**, and **19a,b** were finally converted into final compounds **21**–**26** using the protocol previously described for the introduction of the pendant basic chain.

Starting from **16a,b**, the Meerwein arylation protocol was also

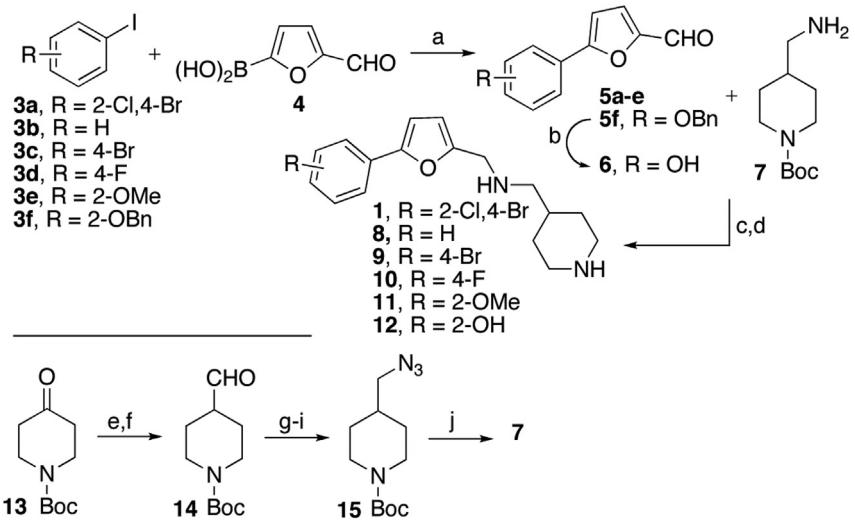

Scheme 1. General synthesis of compounds **1, 8**–**12**.[a]
[a]Reagents and conditions: (a) Bis(triphenylphosphine)Pd(II) dichloride, aq. Na_2CO_3, dimethoxyethane (DME), EtOH, reflux, 12 h, 33–83%; (b) BCl_3, dichloromethane (DCM), −78 °C, 3 h, 55%; (c) i. MeOH, reflux, 12 h; ii. $NaBH_4$, 0 °C, 1 h; (d) 1 N HCl, MeOH, 25 °C, 4 h, 60–75% over two steps; (e) i. $MeOCH_2PPh_3Cl$, $NaN(SiMe_3)_2$, 25 °C, 12 h, 40%; (f) $CeCl_3$, NaI, MeCN, reflux, 12 h, 87%; (g) $NaBH_4$, MeOH, 25 °C, 1 h, 100%; (h) $MeSO_2Cl$, Et_3N, DCM, 25 °C, 12 h, 99%; (i) NaN_3, *N*,*N*-dimethylformamide (DMF), 90 °C, 12 h, 70%; (j) Pd/C, H_2 (1 atm), MeOH, 25 °C, 3 h, 95%.

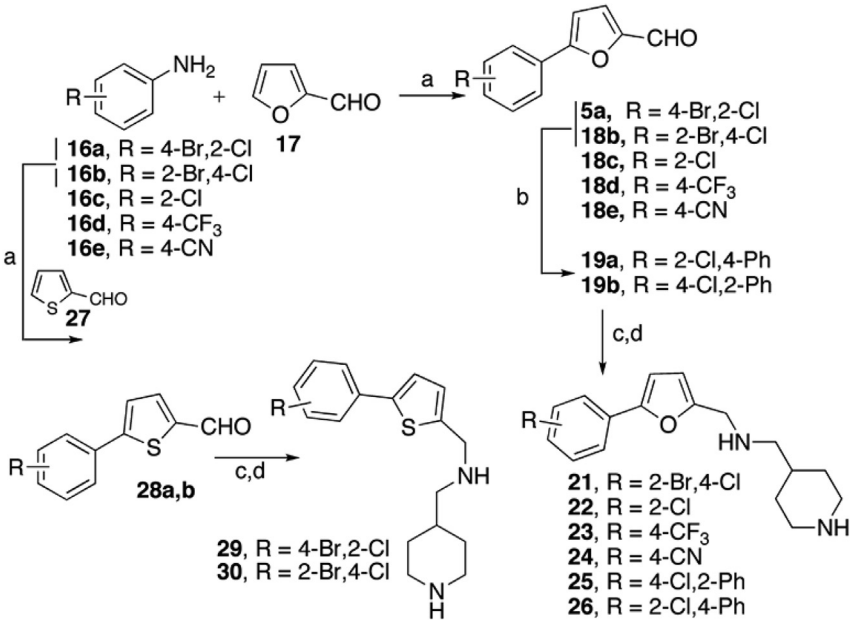

Scheme 2. Synthesis of analogues **21**–**26** and **29,30**.[a]
[a]Reagents and conditions: (a) i. **16a-e**, HCl 37%, $NaNO_2$, H_2O, 0 °C, 1 h; ii. **17** (or **27**), $CuCl_2$, acetone, 25 °C, 12 h, 70–90%; (b) $Pd(OAc)_2$, PPh_3, aq. Na_2CO_3, $PhB(OH)_2$, toluene, reflux, 12 h, 63–85%; (c) i. **7**, MeOH, reflux, 12 h; ii. $NaBH_4$, 0 °C, 1 h; (d) 1 N HCl, MeOH, 25 °C, 4 h, 51–80% over two steps.

applied to the thiophen-carboxaldehyde **27** to obtain intermediates **28a,b**. These latter compounds were then converted to the final compounds **29,30**, representing a first set of analogues of the hit compound **1** bearing modification of the heterocyclic linker.

For the synthesis of the benzothiophene derivative **32** (Scheme 3), aldehyde **31** [33,34] was submitted to the reductive amination reaction, which upon acidic Boc deprotection, led to the preparation of the desired final compound **32**. Compounds bearing five-membered heterocycles **37** and **38** were prepared starting from arylhydrazide **33**. Cyclization of **33** was performed through a Pellizzari-like reaction, consisting in the condensation between acyl hydrazine **33** with benzyl amine [35]. Only the dehalogenated product **34** was obtained from this reaction. The alcoholic function of **35**, introduced by a Prince electrophilic addition using formaldehyde, was activated to the corresponding chloride **36a** which was alkylated with amine **7**. Oxidative *N*-debenzylation [36] followed by acid-mediated deprotection of the Boc-group furnished the triazole **37**. For the synthesis of oxadiazole **38**, the chloromethyl intermediate **36b** was obtained by cyclization of **33** in the presence of chloroacetic acid and $POCl_3$ [37].

Another substitution of the central linker is represented by the pyridine derivative **43** (Scheme 4). A C2 selective Suzuki-Miyaura arylation was applied starting from the commercially available 2-bromo-6-methylpyridine **39** and 4-trifluoromethylphenylboronic

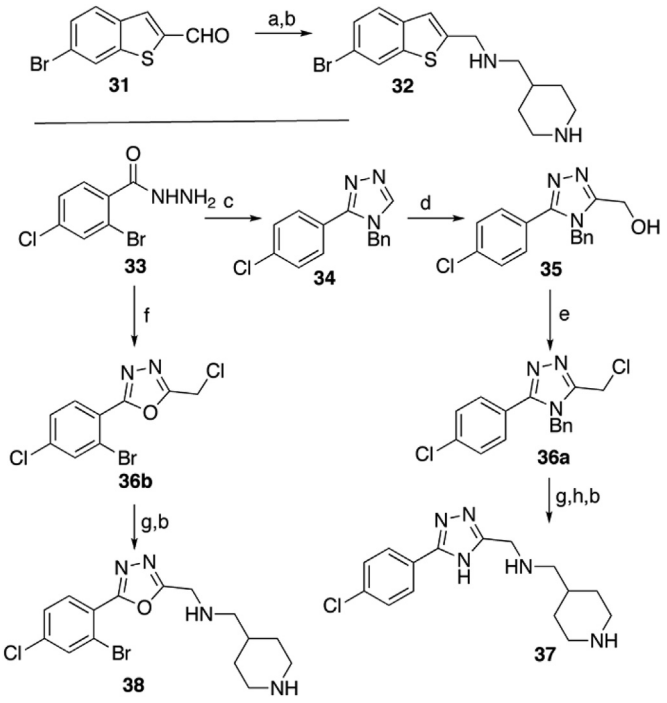

Scheme 3. Synthesis of central linker analogues **32, 37, 38**.[a]
[a]Reagents and conditions: (a) i. **7**, MeOH, reflux, 12 h; ii. $NaBH_4$, 0 °C, 1 h; (b) 1 N HCl, MeOH, 25 °C, 4 h; (c) *N*,*N*-dimethylformamide dimethyl acetal (DMF-DMA), MeCN, 50 °C, 1 h, then $BnNH_2$, AcOH, 120 °C, 12 h, 60%; (d) aq. CH_2O, reflux, 12 h; (e) pyridine, $SOCl_2$, DCM, 0 °C, 3 h, 50%; (f) $POCl_3$, $ClCH_2CO_2H$, reflux, 12 h, 20%; (g) **7**, K_2CO_3, KI (cat.), MeCN, reflux, 1 h, 72%; (h) *t*BuOK, DMSO, THF, O_2, 25 °C, 2 h, 87%.

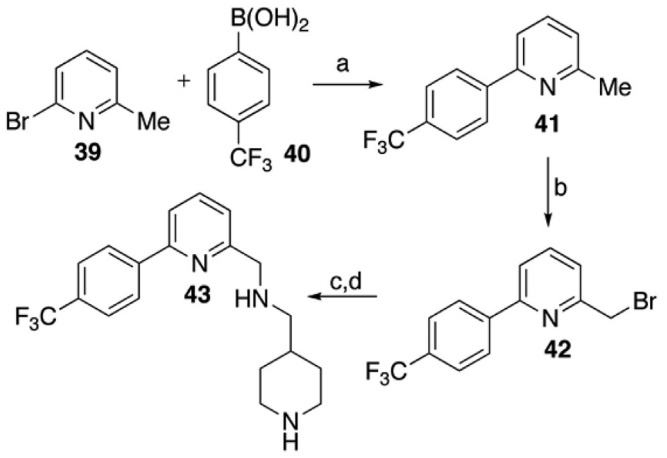

Scheme 4. Synthesis of pyridine derivative **43**.[a]
[a]Reagents and conditions: (a) $Pd(OAc)_2$, PPh_3, K_2CO_3, 7:3 DMF/H_2O, reflux, 12 h, 81%; (b) NBS, AIBN (cat.), CCl_4, reflux, 12 h, 30%; (c) **7**, K_2CO_3, MeCN, reflux, 12 h, 20%; (d) 1 N HCl, MeOH, 25 °C, 4 h, 98%.

acid **40**. The methyl group at C6 of the pyridine ring was then subjected to a bromination reaction using *N*-bromosuccinimide (NBS) and azobisisobutyronitrile (AIBN). The brominated intermediate **42** was used to alkylate amine **7**. The final Boc deprotection gave in high yield the final derivative **43**.

The open-chain analogue **45** was synthesized as described in Scheme 5 starting from intermediate **5a** and the commercially available *N*,*N*′-dimethyl-1,3-propanediamine **44**. Starting from **18b**, reductive amination with **44** followed by protection of the

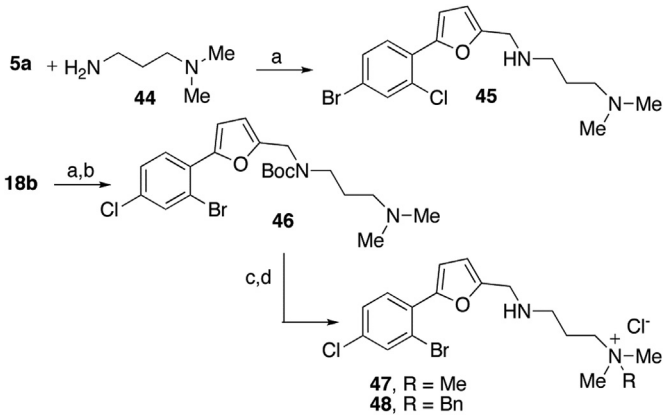

Scheme 5. Synthesis of analogues modified at the protonatable side chain.[a]
[a]Reagents and conditions: (a) i. $NH_2(CH_2)_3NMe_2$, DCM, 25 °C, 1 h; ii. $NaBH(OAc)_3$, 25 °C, 24 h, 85%; (b) $(Boc)_2O$, Et_3N, MeOH, 25 °C, 4 h, 43% over two steps; (c) MeI (for **47**) or BnBr (for **48**), acetone, reflux, 72 h, 58–60%; (d) 1 N HCl, MeOH, 25 °C, 4 h, 94–95%.

secondary amine as Boc-derivative led to intermediate **46**. The tertiary amine was subsequently converted to a quaternary ammonium salt using benzyl bromide and iodomethane, respectively. The final Boc-deprotection using acetyl chloride and methanol gave the two final derivatives **47** and **48** in satisfactory yields.

2.2. Antiplasmodial and gametocytocidal activities and structure-activity relationships

The antiplasmodial activity of the newly synthesized compounds was tested against two laboratory *P. falciparum* strains, the chloroquine-sensitive (CQ-S) D10 and the chloroquine-resistant (CQ-R) W2, according to the described procedures [38,39]. Activity against gametocytes (GCT) was assessed using a luciferase-based assay, as previously described [23].

Selected compounds were also tested against *P. falciparum* strain NF54 asexual blood stage parasites using a Sybrgreen DNA replication assay. NF54 gametocyte assays were performed using reporter strain NF54-HGL [40]. The results of the biological assays are reported in Tables 1–3.

2.2.1. Hydrophobic head

In order to understand if the antiplasmodial and antigametocytocidal activities depended upon the substitution pattern of the aromatic head, we removed one or both alogens of **1** (compounds **9**, **22** and **8**, respectively). Moreover, we inverted the position of the Cl or Br substituent obtaining the regioisomeric derivative **21**, and introduced different electron-withdrawing groups at the *p*-position such as −F (**10**), -CN (**24**), and $-CF_3$ (**23**). We also placed electrondonating and H-bond donor/acceptor groups such as -OMe and −OH (**11** and **12**, respectively). A second aromatic ring, giving rise to regioisomers **25** and **26** was placed along the halogen present in the original structure in order to explore the tolerance of the system to bulky substituents. From this study we derived interesting SARs: as shown in Table 1, the substituents at the hydrophobic head seems to play a key role for *in vitro* activity against both asexual and sexual parasite stages. In particular, the presence of both halogens is important for activity since the unsubstituted analogue **8**, as well as the mono-halogenated derivatives **9**, **10** and **22** are less potent antiplasmodial and gametocytocidal agents than the hit compound **1**. Inversion of chlorine and bromine seems not to have a significant effect on potency as demonstrated by the regioisomeric derivative **21**.

Table 1
Asexual and sexual stages activity (IC_{50}, μM) of compounds modified at the hydrophobic head.

	Structure	D10[a]	W2[b]	GCT: 3D7elo1-pfs16-CBG99	NF54[a]	GCT: NF54-HGL
		IC_{50} (μM)[c]				
1	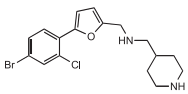	0.77	2.3	1.2	n.t.[d]	n.t.
8	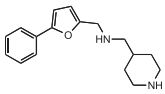	3.5	9.1	8.6	n.t.	n.t.
9	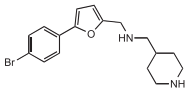	1.1	8.0	4.4	n.t.	n.t.
10	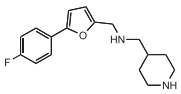	2.1	7.9	6.0	n.t.	n.t.
11	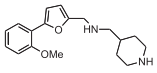	10.0	>15	11.8	n.t.	n.t.
12	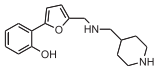	4.4	9.6	8.3	0.26	0.29
21	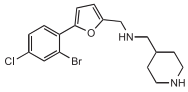	0.51	1.87	1.1	n.t.	n.t.
22	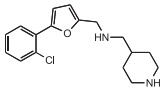	2.1	4.3	5.9	n.t.	n.t.
23	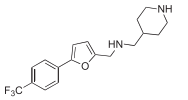	0.41	1.5	1.9	n.t.	n.t.
24	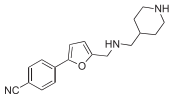	1.1	6.3	18.4	n.t.	n.t.
25	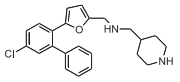	0.88	2.4	1.4	0.67	0.043
26	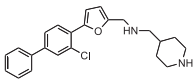	1.0	3.0	1.4	n.t.	n.t.
Chloroquine		0.026	0.31	–	n.t.	–
Epoxomycin		–	–	0.007	–	0.0007
Methylene blue		–	–	0.030	–	n.t.

[a] CQ-S strain.
[b] CQ-R strain.
[c] IC_{50} values are the mean of at least three experiments in duplicate; differences in the experimental conditions, parasite strain/stage, and methods of detection may account for the different IC_{50} observed in the two gametocyte assays. S. D. were within 20% of the mean.
[d] n.t. = not tested.

Among the other electron-withdrawing substituents investigated, the trifluoromethyl derivative **23** maintained a potency similar to **1**, while with a cyano group at para position (**24**) a drop of potency was observed, especially against the gametocytes. Also the introduction of electron-donating substituents such as methoxy (**11**) or hydroxyl (**12**) groups resulted in a dramatic drop of potency against gametocytes. Interestingly, introduction of an aromatic ring at either C2 or C4, as in compounds **25** and **26,** respectively, was tolerated and antiplasmodial and gametocytocidal activities comparable to the hit compound **1** were observed.

2.2.2. Heterocyclic linker

The role of the heterocyclic tether on activity was evaluated through the synthesis of several 5-membered heterocyclic systems

Table 2
Asexual and sexual stages activity (IC_{50}, μM) of compounds modified at the heterocyclic linker.

	Structure	D10[a]	W2[b]	GTC 3D7elo1-pfs16-CBG99	NF54[a]	GTC NF54-HGL
		IC_{50} (μM)[c]				
29	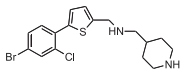	0.73	2.2	0.85	0.28	0.020
30	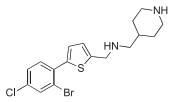	0.53	1.4	0.83	0.42	0.028
32	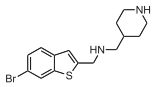	1.0	1.5	1.4	0.73	0.053
37	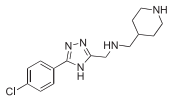	>13	>13	>13	n.t.[d]	n.t.
38	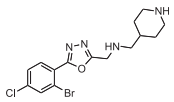	>13	7.9	>26	n.t.	n.t.
43	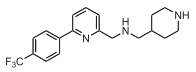	0.46	3.4	4.0	n.t.	n.t.

[a] CQ-S strain.
[b] CQ-R strain.
[c] IC_{50} values are the mean of at least three experiments in duplicate; differences in the experimental conditions, parasite strain/stage, and methods of detection may account for the different IC_{50} observed in the two gametocyte assays. S.D. were within 20% of the mean.
[d] n.t. = not tested.

Table 3
Asexual and sexual stages activity (IC_{50}, μM) of compounds modified at basic side chain.

	Structure	D10[a]	W2[b]	GTC: 3D7elo1-pfs16-CBG99
		IC_{50} (μM)[c]		
45	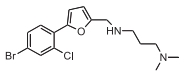	1.2	1.4	1.1
47	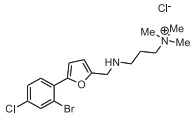	2.5	5.5	>24
48	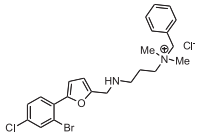	0.55	0.66	4.8

[a] CQ-S strain.
[b] CQ-R strain.
[c] IC_{50} values are the mean of at least three experiments in duplicate. S. D. were within 20% of the mean.

as isosteric derivatives of the furan ring such as thiophene- (**29**, **30**), triazole- (**37**), and oxadiazole- (**38**) derivatives (Table 2). The pyridine-derivative **43** was conceived in order to explore the effect on activity of a 6-membered ring bearing an heteroatom able to function as H-bond acceptor analogously to the furan oxygen, while the fusion of the pendant phenyl ring with the thiophene of **29** resulted in the benzothiophene-derivative **32**. The sulfur-based heterocycles were tolerated and in some cases led to a slight improvement of activity. Also the six-membered pyridine-derivative (**43**) showed reasonable potency, especially against the CQ-S strain, while the other heterocycles investigated led to a dramatic drop of potency.

2.2.3. Pendant basic chain

Derivative **45**, bearing the same basic chain as **2,** showed a potency comparable to **1** (Table 3). The ammonium quaternary salts **47** and **48** were synthesized in an attempt to increase potency since quaternary ammonium salt derivatives were previously displayed as interesting antiplasmodial agents [41]. Both compounds displayed a drop of potency against gametocytes. Interestingly, benzyl derivative **48** maintained its potency against the asexual forms of the parasite, but not against the gametocytes.

For all compounds synthesized, molecular properties calculated *in silico* by QikProp (version 4.3; Schrödinger, LLC: New York, 2015) such as lipophilicity, polar and solvent accessible surface areas, solubility and membrane permeability were all in the recommended range values for known drugs (Table S1 in the Supplementary Information file).

2.3. In vitro cytotoxicity

After investigation of SAR, we selected a representative set of analogues characterized by various degrees of antiplasmodial and gametocytocidal potency for cytotoxicity assays. Cell viability was evaluated *in vitro* against NIH3T3 after 24 h of contact, by Neutral Red Uptake (NRU) test. The cell line has been chosen because is a standard fibroblast cell line.

Results of cytotoxicity tests are reported in Table 4. Compounds **11**, **23** and **25** resulted the least toxic of the series. The reasonable

toxicity of compound **25**, combined to the structure of the inhibitor presenting an extra aromatic ring that could be further decorated, prompted us to select this compound for further biological investigation as detailed in the next paragraphs.

2.4. Standard membrane-feeding assay

The evaluation of the ability of compounds to inhibit the development of oocysts in the mosquito and thus reduce the mosquito's ability to transmit malaria parasites can be confidently assessed using the standard membrane-feeding assay (SMFA) which remains the assay of choice for this kind of investigation. The assay consists in feeding cultured *P. falciparum* gametocytes to *Anopheles* mosquitoes in the presence of the test compound and measuring subsequent mosquito infection. The hit compound **1** was recently shown to have an EC_{50} in the SMFA assay of 0.07 μM [21]. Evaluation of compound **25** in the SMFA assay resulted in an IC_{50} of 0.21 μM on infection intensity, and 0.83 μM on infection prevalence at a baseline infection intensity of 30 oocysts/midgut (Fig. 1). These data confirm that the gametocytocidal activity of **25** as observed in the NF54 gametocyte luciferase assay translates into an inability to infect the mosquito vector. The IC_{50} on infection intensity is slightly higher than expected on basis of the NF54 gametocyte luciferase assay. This may be explained by the difference in incubation time (24 h in the SMFA *vs* 72 h in the gametocyte assay) and a relatively slow mode of action of the compound.

2.5. Evaluation of activity of compound *25* against P. berghei liver stages

We also investigated if compound **25** could have activity against the liver stages of *P. berghei* parasites. Primary mouse hepatocytes have been infected with mCherry expressing *P. berghei* sporozoites. 2 h post infection (hpi) the cells were exposed to different concentrations of **25** for 48 hpi with medium change at 24 hpi. Neither parasite numbers (Fig. 2A) nor parasite sizes (Fig. 2B) were significantly influenced at the concentration tested. Compound **25** was also used to analyze detached cell formation, which is an *in vitro* assay for final development (equivalent to merosome formation *in vivo*). Living parasites were counted at 48 h and from the same wells detached cells at 65 hpi evaluated. Neither concentration tested significantly inhibited detached cell formation, as indicated by the similar rates of detached cells compared to DMSO-treated control cells at 48 h (Fig. 2C).

2.6. Evaluation of cardiac toxicity and calcium antagonist activity of *1* and *25*

Considering the potential *h*ERG liability previously highlighted for compound **1**, we decided to evaluate the cardiotoxic potential of both compounds **1** and **25**. Accordingly, their effect on cardiac mechanical function and electrocardiogram (ECG) in Langendorff-isolated rat hearts was assessed, as previously described [39,42].

Compounds **1** and **25** reduced left ventricular pressure (LVP) in a concentration-dependent manner (Fig. 3), leaving unaltered coronary perfusion pressure (CPP, data not shown). They significantly prolonged atrioventricular conduction time (PQ) and intraventricular conduction time (QRS) in ECG at the maximum concentration tested (10 μM; Table 5). However, QTc values did not vary over the drug range tested (Table 5). Compound **1** significantly decreased heart rate (HR), increased cycle length (RR) interval (Table 5) and caused a sinus arrhythmia in 3 out of 4 hearts.

Since channel blockers, by inhibiting the $Ca_v1.2$ channel currents, may prolong conduction and refractoriness in the atrioventricular node [43], the increased PQ interval obtained in presence of both compounds prompted us to investigate the effects of **1** and **25** on $Ca_v1.2$ channel currents. Compound **1** inhibited $I_{Ba1.2}$ (Ba^{2+} current through $Ca_v1.2$ channels), measured at 0 mV from a holding potential (V_h) of −50 mV, in a concentration-dependent manner (Fig. 4). At 10 μM concentration, inhibition amounted to 57%. Compound **25** blocked the current at 30 μM concentration and showed an IC_{50} value of 3.3 ± 0.5 μM (n = 5).

2.7. In silico approach for target identification of compounds *1* and *25*

Despite recent advances in the field, target identification remains a challenging task that could be approached through several methodologies such as direct biochemical methods, genetic interactions, computational approaches, or a combination of methods. We performed a preliminary computational investigation aimed at identifying a potential target of compounds **1** and **25** from structures in the Protein Data Bank (PDB). As a part of a broad investigation aimed at repurposing FDA-approved drugs against malaria, we prepared all the *P. falciparum* X-ray crystal structures present in PDB at May 2016, to be used in a high-throughput docking (HTD) procedure for identifying potential antimalarial drug-targets targeted by known drugs. Employing a reverse-docking procedure (also known as reverse virtual screening or target fishing) [44], we retrieved from the PDB database (and prepared by Protein Preparation Wizard as previously reported [42,45]) all enzymes and proteins relevant for the plasmodium biology, some of which are established drug targets. Compounds **1** and **25** were then used to "fish" for potential targets by using Glide software [46–48]. The results of our *in silico* study for these compounds indicated a very limited number of potential targets with low docking scores among the examined docking complexes. Surprisingly, for one protein (*P. falciparum* phosphoethanolamine methyltransferase; *Pf*PMT) we observed for both compounds significant docking scores and calculated ligand-binding energies, as found by Glide and Prime (see Experimental part for further details) [46,49–51]. In fact, for **1** and **25** we found computational scores (**1**, Glide XP score = −10.52 kcal/mol, ΔG_{bind} = −57.38 kcal/mol; **25**, Glide XP score = −11.28 kcal/mol, ΔG_{bind} = −67.54 kcal/mol) comparable to those found for sinefungin (Glide XP score = −13.16 kcal/mol, ΔG_{bind} = −84.77 kcal/mol) and *S*-adenosylmethionine (SAM) (Glide XP score = −10.57 kcal/mol, ΔG_{bind} = −82.42 kcal/mol), especially for the docking scores. The most relevant differences were related to the ΔG_{bind}, for which we observed less negative values of **1** and **25** with respect to the reference ligands. So, given the satisfactory *in silico* scores, we decided to test them against PfPMT along with two related derivatives **24** and **48**.

2.7.1. Evaluation of *1, 25* and analogues as inhibitors of PfPMT

Compounds **1**, **24, 25** and **48** were tested as potential inhibitors of *Pf*PMT using a radiochemical assay performed with purified recombinant protein, which was expressed and purified as previously reported (Fig. 5A) [52,53]. Compounds **1**, **24**, and **48** showed weak activity against *Pf*PMT, while compound **25** displayed an inhibitory effect against *Pf*PMT with an IC_{50} = 44.3 ± 5.4 μM (Fig. 5B). The experimental data is in good agreement with the computational

Table 4
Cytotoxic activity against 3T3 cell lines of selected compounds evaluated after 24 h of incubation by NRU test.

Cpd	11	12	21	23	25	26	29	30	45
TC_{50} (μM)[a]	53	7	<5	50	20	5	<5	<5	5

[a] Data are expressed as mean of three experiments repeated in six replicate. S. D.are within 5% of the mean.

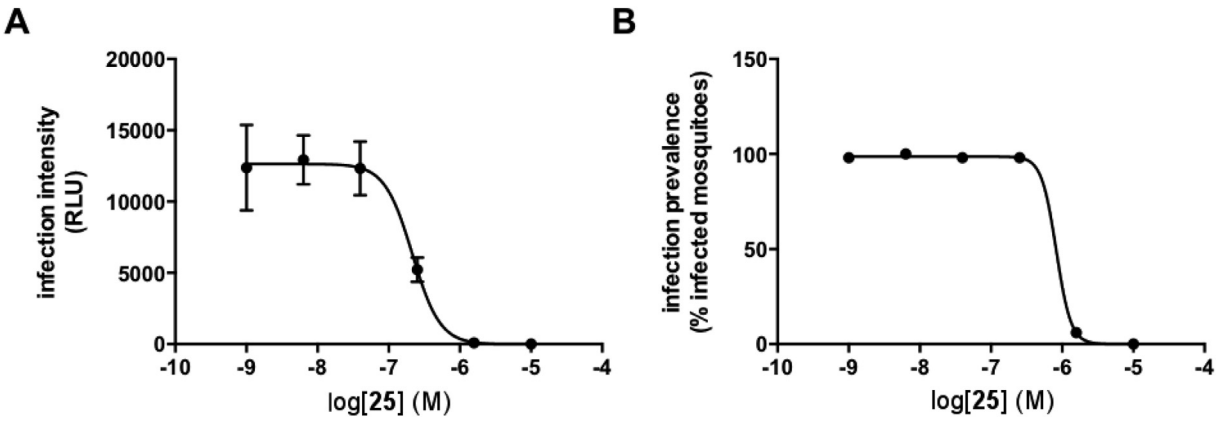

Fig. 1. Compound **25** blocks transmission in the SMFA. A) Compound effect on the infection intensity. The figure shows luminescence activities 8 d post-infection of mosquitoes fed on NF54-HGL gametocytes that were pre-incubated with compound 24 h prior to feeding. A total of 24 mosquitoes was analyzed for each experimental feed, and all feeds were performed in duplicate. The figure shows the mean of the average signal intensities of each feed. Error bars indicate the standard error of the mean B) compound effect of infection prevalence, or the proportion of mosquitoes that carry at least one oocyst. The figure shows average data from two independent feeds. Error bars indicate standard deviations.

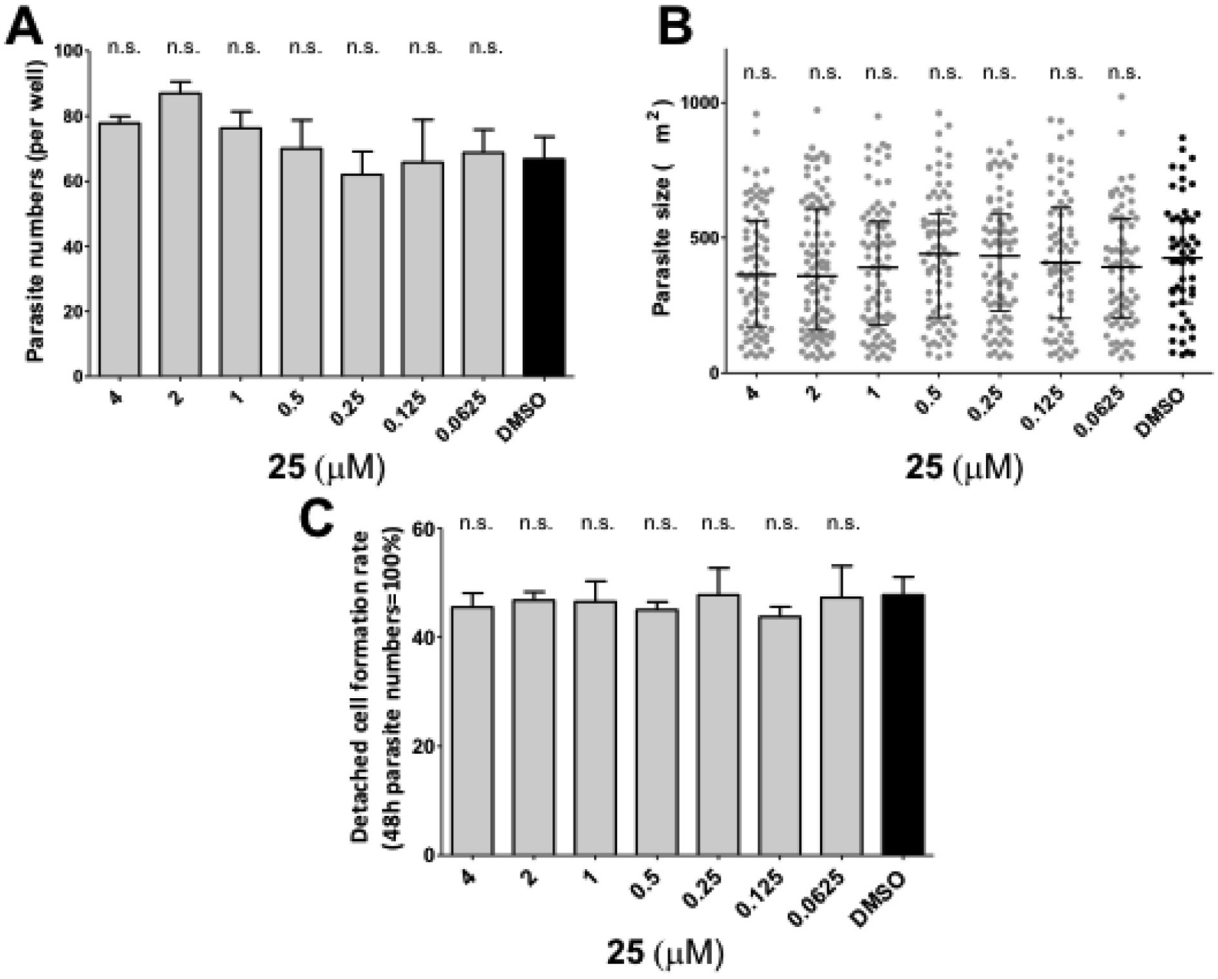

Fig. 2. Compound **25** does not inhibit *P. berghei* liver stage schizont development *in vitro*. Different concentrations of **25** were employed to treat mouse primary hepatocytes infected with mCherry expressing *P. berghei* sporozoites were treated with different concentrations of **25**. **A**. Parasite numbers per well at 48 h are shown (n = 4, SD) indicating no liver stage activity of compound **25**. **B**. Parasite sizes of one replicate of treated cells from A) are shown. **C**. Detached cells compared to DMSO-treated control cells at 48 h One-wayANOVA with Dunnet's Multiple Comparisons (*$p \leq 0.05$, **$p \leq 0.01$ ***$p \leq 0.001$, ns/not significant > 0.05) showed no significant difference compared to the control treated cultures.

output. This latter indicates compound **25** as the best performing compound among the tested molecules, although with slight reduced activity with respect to the reference compounds [53]. Considering that at the moment only few *Pf*PMT inhibitors have been described, mainly related to the natural substrate SAM, compound **25** could be used as a starting point to develop *Pf*PMT

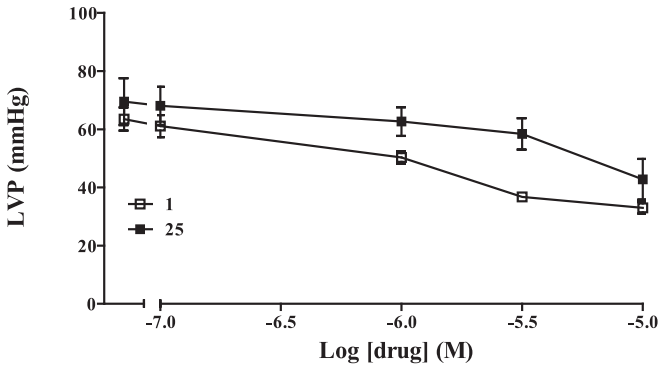

Fig. 3. Effects of **1** and **25** on left ventricular pressure in Langendorff perfused rat hearts. Concentration-effect relationship of **1** and **25** on LVP. On the ordinate scale, response is reported as mmHg. Each value represents mean ± SEM (n = 4 hearts).

inhibitors as potential antimalarials. Fig. 6 depicts the docking output found by Glide software of **25** into the *Pf*PMT active site. In particular, the amino-groups of the compound may form hydrogen bonds with D85 and R127 with the biaryl system fitting into in a hydrophobic sub-pocket and the furan group stacking with H132. Notably, these interactions are part of the main contacts found for the above-mentioned reference compounds [53].

Despite the interesting findings, the inhibition of PfPMT experimentally observed did not correlated with the antiplasmodial and gametocytocidal activity of the compound and from these data we can rule out PfPMT as the target (or at least the main target) of this series of compounds. Our results are in line with a study recently published [25] in which PfPMT has been excluded as the target of **1** in an indirect yeast-mediated assay.

3. Conclusions

Here we described a detailed SAR analysis of hit compound **1** and its analogue **25** for their activity against asexual and sexual life cycle stages of *P. falciparum*. From our SAR studies, the electron withdrawing substituents at the hydrophobic head were identified as important for activity. Moreover, the presence of nitrogen-based heterocyclic linkers resulted detrimental for activity being the thiophene and the furan rings the best performing linkers. A small set of side-chain analogues was explored highlighting that the open-chain analogue retained antiplasmodial potency, while it was interesting to note that among the two quaternary ammonium salts prepared, the benzyl-derivate was active against the asexual life cycle stage. Among the set of compounds synthesized, analogue **25** was selected for a more in depth biological investigation, due to its antiplasmodial potency in the low micromolar range, reasonable cytotoxicity and the presence of an extra aromatic ring that could offer a handle for further scaffold decoration. In particular, compound **25** was active in the SMFA assay with potency comparable to **1**. On the other hand, **25** did not show activity against *P. berghei* hepatocytic life-cycle stage at the concentration tested, even though this could be a species specific effect. Unfortunately, cardiac toxicity was observed for both **1** and **25**. Even though the biological activity of **1** and **25** against gametocytes and asexuals *P. falciparum* stages remains interesting and worth of further investigation, exploitation of this scaffold will only be possible by identifying its target at the molecular level. This is a necessary pre-requisite for investigating if dissociation of *in vitro* toxicity from the specific gametocytocidal and schizontocidal activities is a feasible task. Accordingly, we reported herein our preliminary *in silico* study devoted at identifying the target for this series of compounds. Driven from this study we subsequently found that analogue **25** has an interesting *in vitro* inhibitory activity against *Pf*PMT, a key enzyme for phospholipid biosynthesis in *P. falciparum* [54]. Compound **25** could serve as a starting molecule, for the structure-based design of novel inhibitors as potential antiplasmodial and transmission-blocking agents.

4. Experimental section

4.1. Chemistry

Starting materials and solvents were purchased from commercial suppliers and used without further purification. Reaction progress was monitored by TLC using silica gel 60 F254 (0.040–0.063 mm) with detection by UV. Silica gel 60 (0.040–0.063 mm) was used for column chromatography ^{1}H NMR and ^{13}C NMR spectra were recorded on a Varian 300 MHz, or a Bruker 400 MHz spectrometer using the residual signal of the deuterated solvent as internal standard. Splitting patterns are described as singlet (s), doublet (d), triplet (t), quartet (q), and broad (br); the value of chemical shifts (δ) are given in ppm and coupling constants (J) in Hertz (Hz). Mass spectra were recorded utilizing electron spray ionization (ESI) Agilent 1100 Series LC/MSD spectrometer. Melting points were determined using a Büchi Melting point B-540. Yields refer to purified products and are not optimized. All moisture-sensitive reactions were performed under argon atmosphere using oven-dried glassware and anhydrous solvents. All compounds that were tested in the biological assays were analyzed by combustion analysis (CHN) to confirm the purity > 95%.

4.1.1. 5-(4-Bromo-2-chlorophenyl)furan-2-carbaldehyde (**5a**)

Method A: To a solution of **3a** (150 mg, 0.47 mmol) in a mixture of dry DME (3 mL) and dry EtOH (3 mL), bis(triphenylphosphine) palladium (II) dichloride (17 mg, 0.02 mmol) was added. After 30 min, a solution of sodium carbonate (299 mg, 2.82 mmol) in H_2O (2 mL) and a solution of 5-formyl-2-furanylboronic acid **4** (93 mg, 0.66 mmol) in dry EtOH (1.5 mL) were added in this order. The reaction was heated under reflux for 12 h. After this time, H_2O (4 mL) was added at 25 °C and the organic phase was extracted with EtOAc (3 × 5 mL), dried over sodium sulfate, filtered and evaporated *in vacuo*. The crude product was purified by flash chromatography on silica gel (2% EtOAc in petroleum ether) to give **5a** as orange solid (79 mg, 60%). **Method B:** To a suspension of **16a** (1.0 g, 4.8 mmol) in H_2O (20 mL), HCl (37%, 2 mL) was added. The resulting solution was cooled at 0 °C and a solution of sodium nitrite (397 mg, 5.76 mmol) in H_2O (2 mL) was added dropwise. After 1 h, a solution of **17** (400 μL, 4.8 mmol) in acetone (2 mL) and solid copper (II) chloride (128 mg, 0.96 mmol) were added. The mixture kept at 25 °C for 12 h. EtOAc was added (3 × 10 mL) and the organic phase was separated, dried over sodium sulfate, filtered and evaporated *in vacuo*. The crude product was purified by flash chromatography on silica gel (2% EtOAc in petroleum ether) to give **5a** as orange solid (1.23 g, 90%). mp (EtOAc/*n*-hexane) 141–144 °C; ^{1}H NMR (300 MHz, $CDCl_3$) δ 9.69 (s, 1H), 7.88 (d, J = 8.6 Hz, 1H), 7.65 (s, 1H), 7.50 (d, J = 8.6 Hz, 1H), 7.33 (d, J = 3.8 Hz, 1H), 7.30 (d, J = 3.8 Hz, 1H); ^{13}C NMR (75 MHz, $CDCl_3$) δ 177.6, 154.6, 151.8, 133.7, 132.4, 130.7, 130.2, 126.8, 123.6, 123.0, 113.6. MS (ESI) *m/z* 308 $[M + Na]^+$.

4.1.2. 5-Phenylfuran-2-carbaldehyde (**5b**)

Starting from **3b** (100 mg, 0.49 mmol) and **4** (96 mg, 0.68 mmol), the title compound was prepared following the procedure described for the synthesis of compound **5a (Method A)**. The crude product was purified by flash chromatography on silica gel (5% EtOAc in petroleum ether) to give **5b** as a yellow oil (70 mg, 83%).^{1}H

Table 5
Effects of **1** and **25** on HR, RR, PQ, QRS and QTc in Langendorff perfused rat hearts.[a]

Cpd	(μM)	HR (BPM)	RR (ms)	PQ (ms)	QRS (ms)	QTc (ms)
1	None	247.05 ± 6.87	242.23 ± 5.93	42.63 ± 2.08	14.35 ± 0.47	80.07 ± 1.94
25		275.90 ± 5.43	217.15 ± 3.38	41.13 ± 1.64	13.31 ± 0.62	76.45 ± 1.15
1	0.1	256.15 ± 7.19	235.08 ± 7.41	42.29 ± 2.30	14.25 ± 0.48	81.51 ± 1.95
25		276.19 ± 5.33	218.32 ± 4.37	41.24 ± 1.65	14.20 ± 0.61	74.92 ± 1.01
1	1	258.35 ± 6.79	232.48 ± 6.38	42.50 ± 2.19	15.80 ± 0.39	80.93 ± 1.56
25		275.47 ± 4.14	217.02 ± 3.57	41.59 ± 1.60	13.70 ± 0.43	77.21 ± 2.25
1	3	257.71 ± 7.88	233.90 ± 7.19	47.90 ± 2.95	17.46 ± 1.15	82.10 ± 2.16
25		276.40 ± 3.59	216.73 ± 2.48	45.47 ± 2.58	14.65 ± 0.91	78.56 ± 3.86
1	10	222.74 ± 14.1*	272.57 ± 17.8*	67.50 ± 1.85**	23.75 ± 2.84**	80.99 ± 3.78
25		259.41 ± 6.79	232.20 ± 5.83	65.08 ± 10.15**	17.91 ± 1.33**	83.77 ± 4.58

[a] HR (frequency), RR (cycle length), PQ (atrio-ventricular conduction time), QRS (intraventricular conduction time), QTc (corrected overall action potential duration). Bazett's formula normalized to average rat RR (QTc = QT/(RR/f)1/2) [J. Kmecova, J. Klimas, Heart rate correction of the QT duration in rats, Eur. J. Pharmacol. 641 (2010) 187–192] was used to correct QT. Each value represents mean ± SEM (n = 4 hearts).*P < 0.05,**P < 0.01, repeated measures ANOVA and Dunnett's post test.

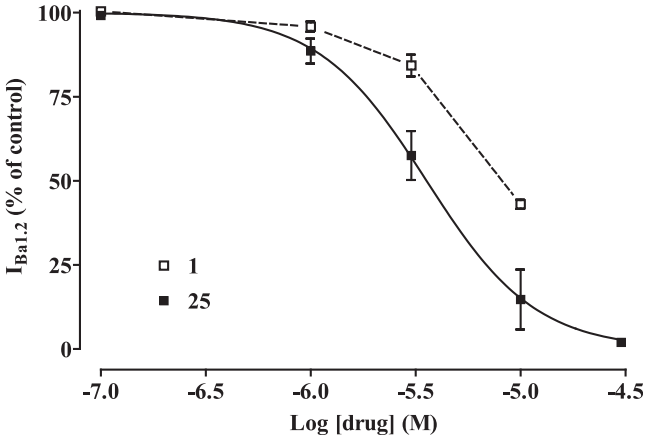

Fig. 4. Effect of compounds **1** and **25** on $I_{Ba1.2}$ in single rat tail artery myocytes. Concentration-dependent effect of **1** and **25** at the peak of $I_{Ba1.2}$ trace. On the ordinate scale, response is reported as percentage of control. Data points are mean ± SEM (n = 3–6 cells, isolated from at least 3 animals).

NMR (400 MHz, $CDCl_3$) δ 9.61 (s, 1H), 7.78 (d, J = 7.6 Hz, 2H), 7.38 (ddd, J = 14.4, 7.9, 4.3 Hz, 3H), 7.28 (d, J = 2.4 Hz, 1H), 6.80 (d, J = 2.4 Hz, 1H); MS (ESI) *m/z* 173 $[M + H]^+$, 195 $[M + Na]^+$.

*4.1.3. 5-(4-Bromophenyl)furan-2-carbaldehyde (**5c**)*

Starting from **3c** (100 mg, 0.35 mmol) and **4** (65 mg, 0.46 mmol), the title compound was prepared following the procedure described for the synthesis of compound **5a (Method A)**. The crude product was purified by flash chromatography on silica gel (5% EtOAc in petroleum ether) to give **5c** as a yellow solid (60 mg, 68%). mp (EtOAc/*n*-hexane) 152–155 °C; ^{1}H NMR (400 MHz, $CDCl_3$) δ 9.62 (s, 1H), 7.63 (d, J = 6.8 Hz, 2H), 7.53 (d, J = 4.8 Hz, 2H), 7.27 (d, J = 3.6 Hz, 1H), 6.80 (d, J = 3.6 Hz, 1H); MS (ESI) *m/z* 252 $[M + H]^+$.

*4.1.4. 5-(4-Fluorophenyl)furan-2-carbaldehyde (**5d**)*

Starting from **3d** (100 mg, 0.45 mmol) and **4** (88 mg, 0.63 mmol), the title compound was prepared following the procedure described for the synthesis of compound **5a (Method A)**. The crude product was purified by flash chromatography on silica gel (5% EtOAc in petroleum ether) to give **5d** as a yellow oil (70 mg, 82%).^{1}H NMR (400 MHz, $CDCl_3$) δ 9.59 (s, 1H), 7.78–7.72 (m, 2H), 7.27 (d, J = 3.5 Hz, 1H), 7.14–7.04 (m, 2H), 6.74 (d, J = 3.4 Hz, 1H); MS (ESI) *m/z* 191 $[M + H]^+$, 213 $[M + Na]^+$.

*4.1.5. 5-(2-Methoxyphenyl)furan-2-carbaldehyde (**5e**)*

Starting from **3e** (160 mg, 0.75 mmol) and **4** (147 mg, 1.05 mmol), the title compound was prepared following the procedure described for the synthesis of compound **5a (Method A)**. The crude product was purified by flash chromatography on silica gel (5% EtOAc in petroleum ether) to give **5e** as a yellow oil (50 mg, 33%). ^{1}H NMR (300 MHz, $CDCl_3$) δ 9.63 (s, 1H), 8.03 (d, J = 5.2 Hz, 1H), 7.40–7.34 (m, 1H), 7.32 (dd, J = 3.8, 1.2 Hz, 1H), 7.12 (dd, J = 3.7, 1.1 Hz, 1H), 7.08–6.96 (m, 2H), 3.93 (s, 3H); MS (ESI) *m/z* 225 $[M + Na]^+$.

*4.1.5.1. 5-(2-Benzyloxyphenyl)furan-2-carbaldehyde (**5f**).* Starting from **3f** (250 mg, 0.80 mmol) and **4** (158 mg, 1.12 mmol), the title compound was prepared following the procedure described for the synthesis of compound **5a (Method A)**. The crude product was purified by flash chromatography on silica gel (5% EtOAc in petroleum ether) to give **5f** as a yellow oil (122 mg, 55%). ^{1}H NMR (300 MHz, $CDCl_3$) δ 9.58 (s, 1H), 8.05 (d, J = 7.8 Hz, 1H), 7.47–7.35 (m, 5H), 7.35–7.26 (m, 1H), 7.26 (d, J = 1.1 Hz, 1H), 7.08–7.01 (m, 3H), 5.14 (s, 2H); MS (ESI) *m/z* 301 $[M + Na]^+$.

*4.1.5.2. 5-(2-Hydroxyphenyl)furan-2-carbaldehyde (**6**).* To a solution of **5f** (122 mg, 0.43 mmol), in dry dichloromethane (DCM) (7 mL), boron trichloride (395 μL, 4.38 mmol) was added at −78 °C. After 3 h, the mixture warmed to 25 °C and the solvent was removed *in vacuo*. The crude product was purified by flash chromatography on silica gel (2% MeOH in DCM) to give **6** as yellow oil (97 mg, 55%). ^{1}H NMR (75 MHz, $CDCl_3$) δ 9.63 (s, 1H), 7.60 (d, J = 6.5 Hz, 1H), 7.26 (d, J = 1.1 Hz, 1H), 7.13–7.08 (m, 1H), 6.92–6.84 (m, 2H), 6.76 (d, J = 3.3 Hz, 1H), 6.28 (d, J = 2.0 Hz, 1H); MS (ESI) *m/z* 189 $[M + H]^+$.

*4.1.6. 1-(5-(4-Bromo-2-chlorophenyl)furan-2-yl)-N-(piperidin-4-ylmethyl)methanamine (**1**)*

A solution of **5a** (90 mg, 0.31 mmol) and **7** (67 mg, 0.31 mmol) in MeOH (10 mL), was heated under reflux for 12 h. After this time, the reaction was cooled to 0 °C and sodium borohydride (12 mg, 0.31 mmol) was added. After 1 h, the solvent was removed *in vacuo*, EtOAc was added (10 mL) and the organic phase was washed with a saturated solution of ammonium chloride (1 × 3 mL), dried over sodium sulfate, filtered and evaporated *in vacuo*. The crude product was purified by flash chromatography on silica gel (2% MeOH in DCM) to give the *N*-Boc protected intermediate as yellow oil (90 mg, 60%). ^{1}H NMR (300 MHz, $CDCl_3$) δ 7.65 (d, J = 8.6 Hz, 1H), 7.53 (d, J = 1.9 Hz, 1H), 7.37 (dd, J = 8.5, 1.9 Hz, 1H), 7.02 (d, J = 3.3 Hz, 1H), 6.27 (d, J = 3.3 Hz, 1H), 4.06 (d, J = 9.6 Hz, 2H), 3.79 (s, 2H), 2.66 (dd, J = 22.1, 9.9 Hz, 2H), 2.50 (d, J = 6.6 Hz, 2H), 1.67 (d, J = 13.0 Hz, 2H), 1.61–1.49 (m, 1H), 1.47–1.36 (m, 9H), 1.08 (d, J = 16.2, Hz, 2H); ^{13}C NMR (75 MHz, $CDCl_3$) δ 155.1, 152.9, 148.9, 133.4, 130.6, 130.3, 128.6, 128.4, 120.6, 112.3, 111.0, 79.5, 59.6, 57.6, 50.8, 34.7, 30.6, 28.7; MS (ESI) *m/z* 506 $[M + Na]^+$. A solution 1 N

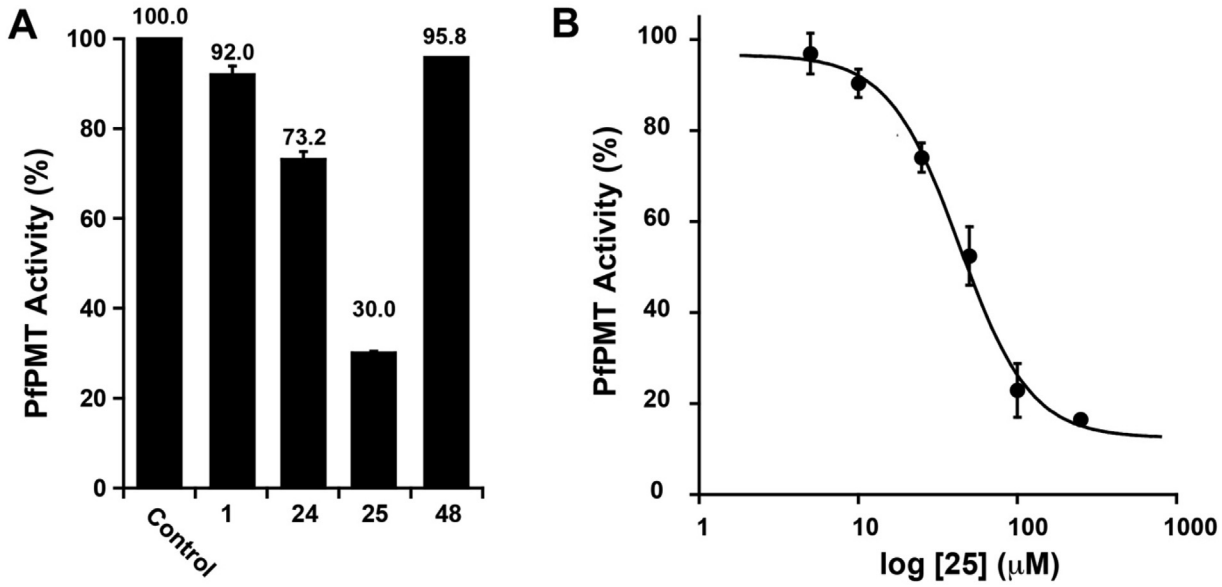

Fig. 5. A. Inhibitory activity against *Pf*PMT by compounds **1**,**24**,**25**,**48** at 100 μM; **B**. *Pf*PMT inhibitory activity ($IC_{50,}$ μM) of **25**. All assays were performed as described in the methods section with values shown as mean ± standard deviation (n = 3).

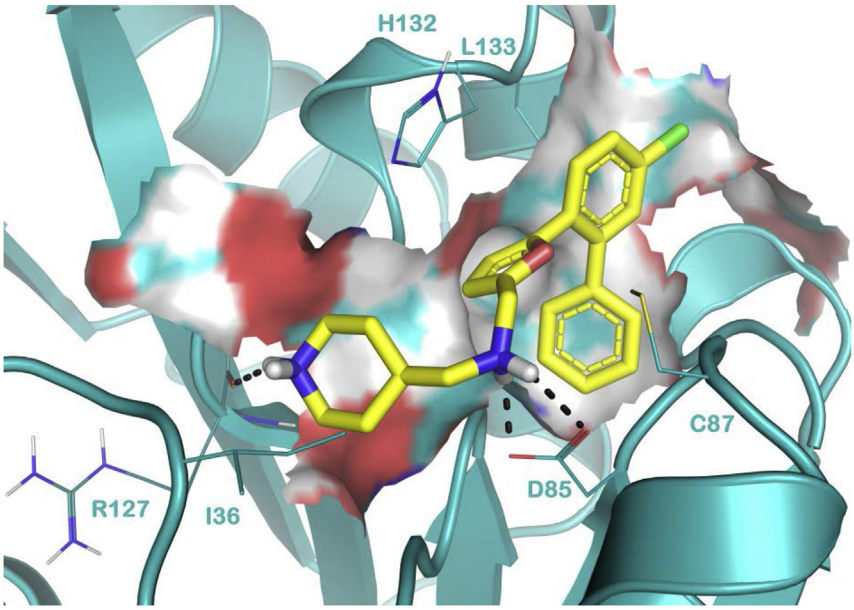

Fig. 6. Putative mode of interaction of compound **25** (yellow sticks) within the active site of *Pf*PMT (deep teal cartoon; PDB ID 3UJ8). H-bonds are represented by black dotted lines. The picture was generated by PyMOL (The PyMOL Molecular Graphics System, v1.8.0; Schrodinger, LLC, New York, 2015). (For interpretation of the references to color in this figure legend, the reader is referred to the Web version of this article.)

HCl was prepared using acetyl chloride (355 μL, 4.97 mmol) in MeOH (4.64 mL). This solution (540 μL, 0.54 mmol) was added to the above described intermediate (90 mg, 0.18 mmol) at 0 °C and the mixture kept at 25 °C for 4 h. The solvent was removed *in vacuo*, a saturated solution of sodium bicarbonate was added and the organic phase was extracted with EtOAc (3 × 4 mL), dried over sodium sulfate, filtered and evaporated *in vacuo*, giving the product **1** as yellow oil without further purification (68 mg, 100%). ^{1}H NMR (300 MHz, CD_3OD) δ 7.88 (d, *J* = 8.5 Hz, 1H), 7.72 (d, *J* = 1.8 Hz, 1H), 7.58 (d, *J* = 6.8 Hz, 1H), 7.19 (d, *J* = 3.3 Hz, 1H), 6.85 (d, *J* = 3.3 Hz, 1H), 4.42 (s, 2H), 3.44 (d, *J* = 12.7 Hz, 2H), 3.05 (dd, *J* = 17.7, 9.1 Hz, 2H), 2.17 (brs, 1H), 2.06 (d, *J* = 14.3 Hz, 2H), 1.55 (dd, *J* = 23.5, 11.6 Hz, 2H); ^{13}C NMR (75 MHz, CD_3OD) δ 150.6, 147.1, 133.1, 130.8, 130.4, 129.2, 127.8, 121.4, 113.7, 112.37, 51.9, 43.9, 43.4, 31.9, 26.4. MS (ESI) *m/z* 383 $[M + H]^+$. Anal. ($C_{17}H_{20}BrClN_2O$) C, H, N.

4.1.7. 1-(5-Phenylfuran-2-yl)-N-piperidin-4-ylmethyl-methanamine (**8**)

Starting from **5b** (30 mg, 0.17 mmol) and **7** (36 mg, 0.17 mmol), the *N*-Boc-protected intermediate was prepared and deprotected as described for the synthesis of **1** to afford **8** as yellow oil (29 mg, 64% over two steps). ^{1}H NMR (400 MHz, $CDCl_3$) δ 7.61 (d, *J* = 7.6 Hz, 2H), 7.34 (t, *J* = 7.6 Hz, 2H), 7.22 (dd, *J* = 12.1, 4.9 Hz, 1H), 6.55 (d, *J* = 3.1 Hz, 1H), 6.23 (d, *J* = 3.1 Hz, 1H), 3.80 (s, 2H), 3.33 (d,

J = 12.5 Hz, 2H), 2.78 (t, J = 11.6 Hz, 2H), 2.56 (d, J = 6.5 Hz, 2H), 1.90 (d, J = 13.5 Hz, 2H), 1.64 (d, J = 3.0 Hz, 1H), 1.54–1.40 (m, 2H); ^{13}C NMR (75 MHz, $CDCl_3$) δ 154.0, 153.3, 131.1, 128.8, 127.3, 123.8, 109.2, 105.8, 55.7, 46.8, 36.8; MS (ESI) m/z 271 $[M + H]^+$. Anal. ($C_{17}H_{22}N_2O$) C, H, N.

4.1.8. 1-(5-(4-Bromophenyl)furan-2-yl)-N-(piperidin-4-ylmethyl) methanamine (**9**)

Starting from **5c** (64 mg, 0.25 mmol) and **7** (53 mg, 0.17 mmol), the *N*-Boc-protected intermediate was prepared and deprotected as described for the synthesis of **1**. The crude product was purified by flash chromatography on silica gel (10% MeOH, 1% NH_4OH, in DCM) to give **9** as yellow oil (38 mg, 64% over two steps). ^{1}H NMR (400 MHz, CD_3OD) δ 7.59 (d, J = 8.5 Hz, 2H), 7.48 (d, J = 8.6 Hz, 2H), 6.78 (d, J = 3.3 Hz, 1H), 6.68 (d, J = 3.2 Hz, 1H), 4.34 (s, 2H), 3.38 (d, J = 12.5 Hz, 2H), 3.02 (d, J = 6.8 Hz, 2H), 2.95 (d, J = 11.4 Hz, 2H), 2.11 (brs, 1H), 2.01 (d, J = 13.6 Hz, 2H), 1.51 (dd, J = 23.4, 11.3 Hz, 2H); ^{13}C NMR (75 MHz, CD_3OD) δ 154.8, 144.8, 131.8, 129.3, 125.6, 121.6, 114.9, 106.8, 51.3, 43.7, 43.2, 31.3, 26.2; MS (ESI) m/z 349 $[M + H]^+$. Anal. ($C_{17}H_{21}BrN_2O$) C, H, N.

4.1.9. 1-(5-(4-Fluorophenyl)furan-2-yl)-N-(piperidin-4-ylmethyl) methanamine (**10**)

Starting from **5d** (32 mg, 0.17 mmol) and **7** (36 mg, 0.17 mmol), the *N*-Boc-protected intermediate was prepared and deprotected as described for the synthesis of **1**. The crude product was purified by flash chromatography on silica gel (10% MeOH, 1% NH_4OH, in DCM) to give **10** as yellow oil (37 mg, 75% over two steps). ^{1}H NMR (400 MHz, CD_3OD) δ 7.76 (d, J = 5.6 Hz, 2H), 7.16 (d, J = 8.7 Hz, 2H), 6.79 (d, J = 3.2 Hz, 1H), 6.74 (d, J = 3.2 Hz, 1H), 4.40 (s, 2H), 3.44 (d, J = 12.1 Hz, 2H), 3.07 (d, J = 6.6 Hz, 2H), 3.00 (d, J = 13.2 Hz, 2H), 2.15 (brs, 1H), 2.04 (d, J = 12.3 Hz, 2H), 1.54 (dd, J = 23.4, 11.3 Hz, 2H); ^{13}C NMR (75 MHz, CD_3OD) δ 164.4, 161.1, 155.0, 144.5, 144.5, 126.8, 126.7, 126.0, 125.9, 115.7, 115.4, 114.9, 105.9, 105.9, 51.3, 43.7, 43.2, 31.3, 26.2; MS (ESI) m/z 289 $[M + H]^+$. Anal. ($C_{17}H_{21}FN_2O$) C, H, N.

4.1.10. 1-(5-(2-Methoxyphenyl)furan-2-yl)-N-(piperidin-4-ylmethyl)methanamine (**11**)

Starting from **5e** (50 mg, 0.25 mmol) and **7** (53 mg, 0.25 mmol), the *N*-Boc-protected intermediate was prepared and deprotected as described for the synthesis of **1**. The crude product was purified by flash chromatography on silica gel (10% MeOH, 1% NH_4OH, in DCM) to give **11** as yellow oil (49 mg, 65% over two steps). ^{1}H NMR (300 MHz, CD_3OD) δ 7.81 (d, J = 7.8 Hz, 1H), 7.22 (t, J = 7.8 Hz, 1H), 7.07–6.94 (m, 2H), 6.84 (d, J = 3.2 Hz, 1H), 6.33 (d, J = 2.6 Hz, 1H), 3.92 (s, 3H), 3.80 (s, 2H), 3.05 (d, J = 12.4 Hz, 2H), 2.61 (t, J = 12.5 Hz, 2H), 2.50 (d, J = 6.6 Hz, 2H), 1.77 (d, J = 13.0 Hz, 2H), 1.65 (m, 1H), 1.21–1.08 (m, 2H); MS (ESI) m/z 301 $[M + H]^+$, 323 $[M + Na]^+$. Anal. ($C_{18}H_{24}N_2O_2$) C, H, N.

4.1.11. 1-(5-(2-Hydroxyphenyl)furan-2-yl)-N-(piperidin-4-ylmethyl)methanamine (**12**)

Starting from **6** (80 mg, 0.42 mmol) and **7** (90 mg, 0.42 mmol), the *N*-Boc-protected intermediate was prepared and deprotected as described for the synthesis of **1**. The crude product was purified by flash chromatography on silica gel (10% MeOH, 1% NH_4OH, in DCM) to give **16** as yellow oil (72 mg, 60% over two steps). ^{1}H NMR (300 MHz, CD_3OD) δ 7.75–7.71 (m, 1H), 7.09–7.02 (m, 1H), 6.91–6.81 (m, 3H), 6.32 (d, J = 2.7 Hz, 1H), 3.78 (s, 2H), 3.00 (d, J = 12.4 Hz, 2H), 2.57 (d, J = 12.2 Hz, 2H), 2.48 (d, J = 6.7 Hz, 2H), 1.72 (d, J = 13.2 Hz, 2H), 1.66–1.55 (m, 1H), 1.21–1.02 (m, 2H); MS (ESI) m/z 287 $[M + H]^+$. Anal. ($C_{17}H_{22}N_2O_2$) C, H, N.

4.1.12. tert-Butyl 4-formylpiperidine-1-carboxylate (**14**)

To a solution of (methoxymethyl)triphenylphosphonium chloride (6.3 g, 18.3 mmol) in dry tetrahydrofuran (THF, 20 mL), sodium bis(trimethylsilyl)amide (1 M in dry THF, 45 mmol) was added dropwise at 0 °C. After 1 h, a solution of **13** (2.8 g, 14.1 mmol) in dry THF (20 mL) was slowly added at 0 °C and the mixture kept at 25 °C for 12 h. The solvent was removed *in vacuo*, H_2O and EtOAc were added and the organic phase was separated, washed with an aqueous solution of HCl 1 N (1 × 5 mL) and with a saturated solution of sodium bicarbonate (1 × 5 mL), dried over sodium sulfate, filtered and evaporated *in vacuo*. The crude reaction mixture was purified by flash chromatography on silica gel (2% EtOAc in petroleum ether) to give the enolether intermediate *tert*-butyl 4-(methoxymethylene)piperidine-1-carboxylate as yellow oil (1.28 g, 40%). ^{1}H NMR (300 MHz, $CDCl_3$) δ 5.81 (s, 1H), 3.51 (s, 3H), 3.33 (t, J = 6.3 Hz, 4H), 2.20 (t, J = 6.0 Hz, 2H), 1.96 (t, J = 6.0 Hz, 2H), 1.42 (s, 9H); MS (ESI) m/z 250 $[M + Na]^+$. To a solution of the above-described compound (807 mg, 3.6 mmol) in CH_3CN (20 mL), cerium chloride (530 mg, 1.4 mmol) and sodium iodide (160 mg, 1.1 mmol) were added. The reaction mixture was heated under reflux for 12 h. The solvent was removed *in vacuo* and the crude product was purified by flash chromatography on silica gel (10% MeOH, 1% NH_4OH, in DCM) to give **14** as yellow oil (667 mg, 87%). ^{1}H NMR (300 MHz, $CDCl_3$) δ 9.57 (s, 1H), 3.88 (d, J = 13.3 Hz, 2H), 2.84 (t, J = 10.9 Hz, 2H), 2.39–2.28 (m, 1H), 1.80 (d, J = 13.5, 2H), 1.49–1.41 (m, 2H), 1.36 (s, 9H). MS (ESI) m/z 268 $[M + MeOH + K]^+$.

4.1.13. tert-Butyl 4-(azidomethyl)piperidine-1-carboxylate (**15**)

To a solution of **14** (660 mg, 3.1 mmol) in MeOH (10 mL), sodium borohydride (117 mg, 3.1 mmol) was added at 0 °C and the mixture kept at 25 °C for 1 h. The solvent was removed in vacuo, EtOAc was added (15 mL) and the organic phase was washed with a saturated solution of ammonium chloride (1 × 5 mL), dried over sodium sulfate, filtered and evaporated *in vacuo*. The alcohol *tert*-butyl 4-(hydroxymethyl)piperidine-1-carboxylate was obtained as yellow oil without further purification (666 mg, 100%). ^{1}H NMR (300 MHz, $CDCl_3$) δ 4.03–3.90 (d, J = 12.6 Hz, 2H), 3.31 (d, J = 6.2 Hz, 2H), 2.56 (t, J = 12.8 Hz, 2H), 1.67–1.54 (m, 2H), 1.54–1.42 (m, 1H), 1.32 (s, 9H), 1.07–0.90 (m, 2H); ^{13}C NMR (75 MHz, $CDCl_3$) δ 154.9, 79.3, 67.6, 67.0, 43.7, 38.8, 38.7, 37.7, 28.4; MS (ESI) m/z 238 $[M + Na]^+$. To a solution of the above-described alcohol (666 mg, 3.1 mmol) in dry DCM (30 mL), triethylamine (2.6 mL, 18.6 mmol) and methanesulfonyl chloride (959 μL, 12.4 mmol) were added dropwise at 0 °C. The reaction mixture was kept at 25 °C for 12 h. A saturated solution of sodium bicarbonate (5 mL) was added and the organic phase was extracted with DCM (3 × 10 mL), dried over sodium sulfate, filtered and evaporated *in vacuo*. The crude product was purified by flash chromatography on silica gel (2% MeOH in DCM) to give mesylate intermediate as yellow oil (900 mg, 99%). ^{1}H NMR (300 MHz, $CDCl_3$) δ 3.98–3.73 (m, 2H), 2.97–2.84 (m, 2H), 2.79 (s, 3H), 2.48 (t, J = 13.1 Hz, 2H), 1.67 (br s, 1H), 1.50 (d, J = 13.2 Hz, 2H), 1.21 (s, 9H), 1.05–0.92 (m, 2H); 13C NMR (75 MHz, CDCl3) δ 154.8, 79.6, 73.7, 43.3, 37.3, 36.0, 31.8, 28.5, 28.3; MS (ESI) m/z 294 [M + H]+. To a solution of the above compound (900 mg, 3.1 mmol) in dry *N*,*N*-dimethylformamide (DMF) (10 mL), sodium azide (400 mg, 6.2 mmol) was added at 0 °C. The reaction was heated under reflux at 90 °C for 12 h. The solvent was removed *in vacuo* and the product 15 was obtained as yellow oil without further purification (0.52 g, 70%). ^{1}H NMR (300 MHz, $CDCl_3$) δ 4.01 (d, J = 12.1 Hz, 2H), 3.08 (d, J = 6.3 Hz, 2H), 2.57 (t, J = 12.8 Hz, 2H), 1.68–1.49 (m, 3H), 1.34 (s, 9H), 1.15–0.96 (m, 1H); ^{13}C NMR (75 MHz, $CDCl_3$) δ 111.3, 79.7, 57.2, 43.4, 36.7, 29.8, 28.6; MS (ESI) m/z 263 [M + Na]+.

4.1.14. tert-Butyl 4-(aminomethyl)piperidine-1-carboxylate (**7**)

To a solution of **15** (520 mg, 2.1 mmol) in MeOH (15 mL), a catalytic amount of palladium on carbon 10 wt.% was added under

argon atmosphere. The reaction environment was saturated with hydrogen gas. The mixture was stirred at 25 °C for 3 h. The suspension was filtered on paper and concentrated *in vacuo* giving **7** as colorless oil without further purification (427 mg, 95%). ^{1}H NMR (300 MHz, $CDCl_3$) δ 3.88 (d, J = 13.1 Hz, 2H), 2.50 (d, J = 17.4 Hz, 4H), 2.45–2.33 (m, 2H), 1.50 (d, J = 13.0 Hz, 2H), 1.38–1.27 (m, 1H), 1.27 (s, 9H), 0.90–0.45 (m, 2H); ^{13}C NMR (75 MHz, $CDCl_3$) δ 155.0, 79.3, 48.1, 43.4, 39.7, 29.9, 28.6; MS (ESI) *m/z* 215 $[M + H]^+$.

4.1.15. 5-(4-Chloro-2-bromophenyl)furan-2-carbaldehyde (**18b**)

Starting from **16b** (2.0 g, 9.7 mmol) and **17** (802 μL, 9.7 mmol), the title compound was prepared following the procedure described for the synthesis of compound **5a (Method B)**. The crude product was purified by flash chromatography on silica gel (5% EtOAc in petroleum ether) to give **18b** as an orange solid (2.5 g, 90%). mp (EtOAc/*n*-hexane)141–144 °C; ^{1}H NMR (300 MHz, $CDCl_3$) δ 9.69 (s, 1H), 7.89 (d, J = 8.5 Hz, 1H), 7.71 (d, J = 2.0 Hz, 1H), 7.40 (d, J = 8.6, Hz, 1H), 7.35 (q, J = 3.8 Hz, 2H); ^{13}C NMR (75 MHz, $CDCl_3$) δ 177.6, 154.6, 151.8, 133.7, 132.4, 130.7, 130.2, 126.8, 123.6, 123.0, 113.6. MS (ESI) *m/z* 308 $[M + Na]^+$.

4.1.16. 5-(2-Chlorophenyl)furan-2-carbaldehyde (**18c**)

Starting from **16c** (100 mg, 0.78 mmol) and **17** (65 μL, 0.78 mmol), the title compound was prepared following the procedure described for the synthesis of compound **5a (Method B)**. The crude product was purified by flash chromatography on silica gel (10% EtOAc in petroleum ether) to give **18c** as a yellow solid (112 mg, 70%). mp (EtOAc/*n*-hexane) 68–72 °C; ^{1}H NMR (400 MHz, $CDCl_3$) δ 9.66 (s, 1H), 7.97 (d, J = 5.9 Hz, 1H), 7.44 (d, J = 6.5 Hz, 1H), 7.36–7.26 (m, 4H); MS (ESI) *m/z* 207 $[M + H]^+$, 228 $[M + Na]^+$.

4.1.17. 5-(4-(Trifluoromethyl)phenyl)furan-2-carbaldehyde (**18d**)

Starting from **16d** (300 mg, 1.86 mmol) and furaldehyde **17** (154 μL, 1.86 mmol), the title compound was prepared following the procedure described for the synthesis of compound **5a (Method B)**. The crude product was purified by flash chromatography on silica gel (5% EtOAc in petroleum ether) to give **18d** as yellow solid (312 mg, 70%). mp (EtOAc/*n*-hexane) 64–66 °C; ^{1}H NMR (300 MHz, $CDCl_3$) δ 9.65 (s, 1H), 7.85 (d, J = 8.6 Hz, 2H), 7.64 (d, J = 8.6 Hz, 2H), 7.30 (d, J = 3.8 Hz, 1H), 6.91 (d, J = 3.8 Hz, 1H); MS (ESI) *m/z* 263 $[M + Na]^+$.

4.1.18. 4-(5-Formylfuran-2-yl)benzonitrile (**18e**)

Starting from **16e** (600 mg, 5.1 mmol) and furaldehyde **17** (421 μL, 1.86 mmol), the title compound was prepared following the procedure described for the synthesis of compound **5a (Method B)**. The crude product was purified by flash chromatography on silica gel (15% EtOAc in petroleum ether) to give **18e** as brown solid (753 mg, 75%). mp (EtOAc/*n*-hexane) 145–150 °C; ^{1}H NMR (300 MHz, $CDCl_3$) δ 9.71 (s, 1H), 7.92 (d, J = 8.6 Hz, 2H), 7.76 (d, J = 8.6 Hz, 2H), 7.34 (d, J = 3.4 Hz, 1H), 6.97 (d, J = 3.4 Hz, 1H); MS (ESI) *m/z* 220 $[M + Na]^+$.

4.1.19. 5-(4-Phenyl-2-chlorophenyl)furan-2-carbaldehyde (**19a**)

Triphenylphosphine (220 mg, 0.84 mmol) and palladium (II) acetate (12 mg, 0.05 mmol) were dissolved in dry toluene (3 mL) under argon atmosphere. After 30 min, a solution of **5a** (300 mg, 1.05 mmol) in dry toluene (5 mL) was added. After further 30 min, a solution of sodium carbonate (701 mg, 6.6 mmol) in H_2O (3 mL) and powdered phenyl boronic acid (128 mg, 1.05 mmol) were added in this order. Reaction was heated under reflux for 12 h. The solvent was removed under *vacuo*. H_2O (2 mL) and EtOAc (8 mL) were added, the organic phase was separated, dried over sodium sulfate, filtered and evaporated *in vacuo*. The crude product was purified by flash chromatography on silica gel (5% EtOAc in petroleum ether) to give **19a** as yellow oil (254 mg, 85%). ^{1}H NMR (300 MHz, $CDCl_3$) δ 9.69 (s, 1H), 8.08 (d, J = 1.5 Hz, 1H), 7.70 (d, J = 1.6 Hz,1H), 7.62–7.56 (m, 3H), 7.50–7.36 (m, 3H), 7.35 (d, J = 0.8 Hz, 2H); ^{13}C NMR (75 MHz, $CDCl_3$) δ 177.6, 157.7, 151.5, 142.6, 140.0, 135.4, 131.1, 129.8, 129.4, 129.0 (2C), 127.5, 127.3, 126.4 (2C), 115.6, 112.3; MS (ESI) *m/z* 305 $[M + Na]^+$.

4.1.20. 5-(2-Phenyl-4-chlorophenyl)furan-2-carbaldehyde (**19b**)

Starting from **18b** (80 mg, 0.28 mmol) and phenylboronic acid (35 mg, 0.28 mmol), the title compound was prepared following the procedure reported for compound **19a**. The crude product was purified by flash chromatography on silica gel (5% EtOAc in petroleum ether) to give **19b** as yellow oil (50 mg, 63%). ^{1}H NMR (300 MHz, $CDCl_3$) δ 9.55 (s, 1H), 7.93 (d, J = 5.3 Hz, 1H), 7.44–7.40 (m, 5H), 7.33 (d, J = 2.7 Hz, 2H), 7.02 (d, J = 3.1 Hz, 1H), 5.62 (d, J = 3.7 Hz, 1H); ^{13}C NMR (75 MHz, $CDCl_3$) δ 177.6, 157.7, 151.5, 142.6, 140.0, 135.4, 131.1, 129.8, 129.4, 129.0 (2C), 127.5, 127.4, 126.4, 120.4, 115.6, 112.3; MS (ESI) *m/z* 305 $[M + Na]^+$.

4.1.21. 1-(5-(2-Bromo-4-chlorophenyl)furan-2-yl)-N-(piperidin-4-ylmethyl)methanamine (**21**)

Starting from **18b** (50 mg, 0.18 mmol) and **7** (38 mg, 0.18 mmol), the *N*-Boc-protected intermediate was prepared and deprotected as described for the synthesis of **1**. The crude product was purified by flash chromatography on silica gel (10% MeOH, 1% NH_4OH, in DCM) to give **21** as yellow oil (48 mg, 70% over two steps). ^{1}H NMR (300 MHz, $CDCl_3$) δ 7.65 (d, J = 1.2 Hz, 1H), 7.61 (s, 1H), 7.28 (d, J = 2.2 Hz, 1H), 7.05 (s, 1H), 6.27 (s, 1H), 3.78 (s, 2H), 3.30 (d, J = 11.1 Hz, 2H), 2.74 (t, J = 11.8 Hz, 2H), 2.53 (d, J = 5.2 Hz, 2H), 1.86 (d, J = 12.9 Hz, 2H), 1.61 (s, 1H), 1.48–1.30 (m, 2H); ^{13}C NMR (75 MHz, CD_3OD) δ 153.7, 149.5, 133.1, 132.9, 129.8, 129.1, 127.5, 118.9, 111.5, 109.2, 54.3, 45.3, 44.7, 34.9, 29.2; MS (ESI) *m/z* 383 $[M + H]^+$. Anal. ($C_{17}H_{20}BrClN_2O$) C, H, N.

4.1.22. 1-(5-(2-Chlorophenyl)furan-2-yl)-N-(piperidin-4-ylmethyl) methanamine (**22**)

Starting from **18c** (45 mg, 0.22 mmol) and **7** (47 mg, 0.22 mmol), the *N*-Boc-protected intermediate was prepared and deprotected as described for the synthesis of **1**. The crude product was purified by flash chromatography on silica gel (10% MeOH, 1% NH_4OH, in DCM) to give **22** as yellow oil (48 mg, 68% over two steps). ^{1}H NMR (300 MHz, CD_3OD) δ 7.91 (dd, J = 7.8, 1.7 Hz, 1H), 7.51–7.47 (m, 1H), 7.41–7.26 (m, 2H), 7.12 (d, J = 3.5 Hz, 1H), 6.75 (d, J = 3.5 Hz, 1H), 4.32 (s, 2H), 3.40 (d, J = 2.4 Hz, 2H), 3.30 (dt, J = 2.3, 1.6 Hz, 2H), 3.04–2.94 (m, 2H), 2.15–2.07 (m, 1H), 2.02 (d, J = 14.3 Hz, 2H), 1.52 (td, J = 14.7, 4.0 Hz, 2H); ^{13}C NMR (75 MHz, CD_3OD) δ 151.7, 146.3, 130.7, 130.2, 129.0, 128.6, 128.2, 127.1, 113.8, 111.8, 51.7, 43.9, 43.3, 31.7, 26.4; MS (ESI) *m/z* 305 $[M + H]^+$. Anal. ($C_{17}H_{21}ClN_2O$) C, H, N.

4.1.23. 1-(5-(4-Trifluoromethylphenyl)furan-2-yl)-N-(piperidin-4-ylmethyl)methanamine (**23**)

Starting from **18d** (100 mg, 0.41 mmol) and **7** (89 mg, 0.41 mmol), the *N*-Boc-protected intermediate was prepared and deprotected as described for the synthesis of **1**. The crude product was purified by flash chromatography on silica gel (10% MeOH, 1% NH_4OH, in DCM) to give **23** as yellow oil (90 mg, 65% over two steps). ^{1}H NMR (300 MHz, CD_3OD) δ 7.86 (d, J = 8.1 Hz, 2H), 7.66 (d, J = 7.6 Hz, 2H), 6.89 (d, J = 3.3 Hz, 1H), 6.42 (d, J = 3.3 Hz, 1H), 3.83 (s, 2H), 3.16 (d, J = 11.7 Hz, 2H), 2.72 (t, J = 12.4 Hz, 2H), 2.53 (d, J = 6.3 Hz, 2H), 1.85 (d, J = 14.0 Hz, 2H), 1.70 (brs, 1H), 1.28–1.15 (m, 2H); ^{13}C NMR (75 MHz, CD_3OD) δ 154.3, 151.6, 134.2, 128.5, 128.1, 125.4, 125.3, 125.3, 125.2, 123.3, 109.7, 107.8, 54.6, 45.3, 45.1, 35.4, 30.0; MS (ESI) *m/z* 338 $[M + H]^+$. Anal. ($C_{18}H_{21}F_3N_2O$) C, H, N.

*4.1.24. 1-(5-(4-Cyanophenyl)furan-2-yl)-N-(piperidin-4-ylmethyl) methanamine (**24**)*

Starting from **18e** (51 mg, 0.26 mmol) and **7** (55 mg, 0.41 mmol), the *N*-Boc-protected intermediate was prepared and deprotected as described for the synthesis of **1**. The crude product was purified by flash chromatography on silica gel (10% MeOH, 1% NH_4OH, in DCM) to give **24** as yellow oil (51 mg, 67% over two steps). ^1H NMR (300 MHz, CD_3OD) δ 7.88 (d, $J = 8.6$ Hz, 2H), 7.72 (d, $J = 8.6$ Hz, 2H), 7.03 (d, $J = 3.5$ Hz, 1H), 6.77 (d, $J = 3.5$ Hz, 1H), 4.41 (s, 2H), 3.47–3.37 (m, 2H), 3.08 (t, $J = 7.7$ Hz, 2H), 3.02–2.93 (m, 2H), 2.14 (brs, 1H), 2.08–2.00 (m, 2H), 1.51 (dd, $J = 18.7$, 8.6 Hz, 2H); ^{13}C NMR (75 MHz, CD_3OD) δ 153.7, 146.3, 134.2, 132.6, 131.9, 124.4, 118.5, 115.15, 110.6, 109.4, 51.4, 43.6, 43.2, 31.3, 26.2; MS (ESI) *m/z* 296 $[M + H]^+$. Anal. ($C_{18}H_{21}N_3O$) C, H, N.

*4.1.25. 1-(5-(2-Phenyl-4-chlorophenyl)furan-2-yl)-N-(piperidin-4-ylmethyl)methanamine (**25**)*

Starting from **19b** (50 mg, 0.17 mmol) and **7** (38 mg, 0.17 mmol), the *N*-Boc-protected intermediate was prepared and deprotected as described for the synthesis of **1**. The crude product was purified by flash chromatography on silica gel (10% MeOH, 1% NH_4OH, in DCM) to give **25** as yellow oil (52 mg, 80% over two steps). ^1H NMR (300 MHz, CD_3OD) δ 7.76 (d, $J = 8.5$ Hz, 1H), 7.43–7.35 (m, 4H), 7.27–7.21 (m, 3H), 6.10 (d, $J = 3.1$ Hz, 1H), 5.60 (d, $J = 3.3$ Hz, 1H), 3.63 (s, 2H), 3.05 (d, $J = 12.4$ Hz, 2H), 2.60 (t, $J = 11.7$ Hz, 2H), 2.39 (d, $J = 6.7$ Hz, 2H), 1.72 (d, $J = 13.0$ Hz, 2H), 1.64–1.53 (m, 1H), 1.20–1.04 (m, 2H); ^{13}C NMR (75 MHz, CD_3OD) δ 171.8, 152.7, 151.4, 141.1, 141.1, 132.7, 130.3, 128.7, 128.4, 128.2, 127.6, 127.5, 110.0, 109.2, 53.7, 45.3, 44.0, 33.9, 27.4; MS (ESI) *m/z* 381 $[M + H]^+$. Anal. for ($C_{23}H_{25}ClN_2O$) C, H, N.

*4.1.26. 1-(5-(4-Phenyl-2-chlorophenyl)furan-2-yl)-N-(piperidin-4-ylmethyl)methanamine (**26**)*

Starting from **19a** (50 mg, 0.17 mmol) and **7** (38 mg, 0.17 mmol), the *N*-Boc-protected intermediate was prepared and deprotected as described for the synthesis of **1**. The crude product was purified by flash chromatography on alumina gel (2% MeOH, 0.5% NH_4OH, in DCM) to give **26** as yellow oil (33 mg, 51% over two steps). ^1H NMR (300 MHz, CD_3OD) δ 7.97 (d, $J = 8.3$ Hz, 1H), 7.72 (d, $J = 1.9$ Hz, 1H), 7.68–7.60 (m, 3H), 7.54–7.34 (m, 3H), 7.11 (d, $J = 3.3$ Hz, 1H), 6.44 (d, $J = 3.3$ Hz, 1H), 3.84 (s, 2H), 3.06 (d, $J = 12.2$ Hz, 2H), 2.61 (t, $J = 11.6$ Hz, 2H), 2.52 (d, $J = 6.9$ Hz, 2H), 1.78 (d, $J = 13.6$ Hz, 2H), 1.66 (brs, 1H), 1.25–1.08 (m, 2H); ^{13}C NMR (75 MHz, $CDCl_3$) δ 154.3, 149.4, 140.9, 139.4, 133.4, 130.4, 130.3, 129.3, 129.1, 128.8, 128.2, 128.1, 127.1, 125.6, 112.0, 109.4, 55.7, 46.8, 46.7, 36.8, 31.6; MS (ESI) *m/z* 381 $[M + H]^+$. Anal. for ($C_{23}H_{25}ClN_2O$) C, H, N.

*4.1.27. 5-(4-Bromo-2-chlorophenyl)thiophene-2-carbaldehyde (**28a**)*

Starting from **16a** (300 mg, 1.5 mmol) and **27** (135 μL, 1.5 mmol), the title compound was prepared following the procedure described for the synthesis of compound **5a (Method B)**. The crude product was purified by flash chromatography on silica gel (10% EtOAc in petroleum ether) to give **28a** as yellow oil (360 mg, 80%). ^1H NMR (300 MHz, $CDCl_3$) δ 9.93 (s, 1H), 7.75 (d, $J = 3.9$ Hz, 1H), 7.72 (d, $J = 2.0$ Hz, 1H), 7.41 (s, 1H), 7.38–7.35 (m, 2H); ^{13}C NMR (75 MHz, $CDCl_3$) δ 183.1, 148.7, 144.2, 136.3, 133.5, 133.5, 132.4, 131.1, 130.7, 129.1, 123.5; MS (ESI) *m/z* 302 $[M + H]^+$.

*4.1.28. 5-(2-Bromo-4-chlorophenyl)thiophene-2-carbaldehyde (**28b**)*

Starting from **16b** (200 mg, 0.97 mmol) and **27** (87 μL, 0.97 mmol), the title compound was prepared following the procedure described for the synthesis of compound **5a (Method B)**. The crude product was purified by flash chromatography on silica gel (10% EtOAc in petroleum ether) to give **28b** as yellow oil (227 mg, 78%). ^1H NMR (300 MHz, $CDCl_3$) δ 9.93 (s, 1H), 7.75 (d, $J = 3.9$ Hz, 1H), 7.72 (d, $J = 2.0$ Hz, 1H), 7.41 (s, 1H), 7.38–7.35 (m, 2H). ^{13}C NMR: (75 MHz, $CDCl_3$) δ 183.1, 148.7, 144.2, 136.3, 133.5, 133.5, 132.4, 131.1, 130.7, 129.1, 123.5. MS (ESI) *m/z* 302 $[M + H]^+$.

*4.1.29. 1-(5-(4-Bromo-2-chlorophenyl)thiophen-2-yl)-N-(piperidin-4-ylmethyl)methanamine (**29**)*

Starting from **28a** (88 mg, 0.4 mmol) and **7** (85 mg, 0.4 mmol), the *N*-Boc-protected intermediate was prepared and deprotected as described for the synthesis of **1**. The crude product was purified by flash chromatography on silica gel (10% MeOH, 1% NH_4OH, in DCM) to give **29** as yellow oil (115 mg, 72% over two steps). ^1H NMR (300 MHz, $CDCl_3$) δ 7.62 (s, 1H), 7.38 (d, $J = 1.6$ Hz, 1H), 7.26 (d, $J = 0.9$ Hz, 1H), 7.20 (d, $J = 2.4$ Hz, 1H), 6.90 (d, $J = 2.7$ Hz, 1H), 3.98 (s, 2H), 3.08 (d, $J = 12.2$ Hz, 2H), 2.57 (d, $J = 6.5$ Hz, 2H), 1.74 (m, 4H), 1.61 (brs, 2H), 1.29–1.07 (m, 3H); ^{13}C NMR (75 MHz, $CDCl_3$) δ 207.2, 146.4, 137.9, 133.2, 132.6, 132.3, 130.3, 127.8, 125.0, 121.4, 55.6, 49.0, 46.3, 36.6, 31.1; MS (ESI) *m/z* 400 $[M + H]^+$. Anal. ($C_{17}H_{20}BrClN_2S$) C, H, N.

*4.1.30. 1-(5-(2-Bromo-4-chlorophenyl)thiophen-2-yl)-N-(piperidin-4-ylmethyl)methanamine (**30**)*

Starting from **28b** (48 mg, 0.2 mmol) and **7** (43 mg, 0.2 mmol), the *N*-Boc-protected intermediate was prepared and deprotected as described for the synthesis of **1**. The crude product was purified by flash chromatography on silica gel (10% MeOH, 1% NH_4OH, in DCM) to give **30** as yellow oil (50 mg, 63% over two steps). ^1H NMR (300 MHz, CD_3OD) δ 7.73 (s, 1H), 7.46 (d, $J = 8.4$ Hz, 1H), 7.40–7.37 (m, 1H), 7.14 (d, $J = 1.5$ Hz, 1H), 6.98 (d, $J = 2.7$ Hz, 1H), 3.95 (s, 2H), 3.06 (d, $J = 12.8$ Hz, 2H), 2.62 (t, $J = 13.3$, Hz, 2H), 2.51 (d, $J = 6.6$ Hz, 2H), 1.78 (d, $J = 13.2$ Hz, 2H), 1.65 (m, 1H), 1.28–1.08 (m, 2H); ^{13}C NMR (75 MHz, $CDCl_3$) δ 207.2, 146.4, 137.9, 133.2, 132.6, 132.29, 130.3, 127.8, 125.0, 121.4, 55.6, 49.0, 46.3, 36.6, 31.1; MS (ESI) *m/z* 400 $[M + H]^+$. Anal. ($C_{17}H_{20}BrClN_2S$) C, H, N.

*4.1.31. 1-(5-Bromobenzothiophen-2-yl)-N-(piperidin-4-ylmethyl) methanamine (**32**)*

Starting from **31** (40 mg, 0.21 mmol), the *N*-Boc-protected intermediate was prepared and deprotected as described for the synthesis of **1**. The crude product was purified by flash chromatography on silica gel (10% MeOH, 1% NH_4OH, in DCM) to give **32** as yellow oil (41 mg, 60% over two steps). ^1H NMR (300 MHz, CD_3OD) δ 7.97 (s, 1H), 7.61 (d, $J = 8.5$ Hz, 1H), 7.41 (d, $J = 4.2$, Hz, 1H), 7.20 (s, 1H), 4.01 (s, 2H), 3.03 (d, $J = 12.4$ Hz, 2H), 2.58 (t, $J = 12.4$, Hz, 2H), 2.49 (d, $J = 6.7$ Hz, 2H), 1.75 (d, $J = 13.2$ Hz, 2H), 1.71–1.56 (m, 1H), 1.13 (m, 2H); ^{13}C NMR (75 MHz, CD_3OD) δ 145.9, 141.6, 138.9, 127.4, 124.5, 124.3, 121.5, 117.3, 54.8, 45.4, 35.9, 30.4; MS (ESI) *m/z* 362 $[M + Na]^+$. Anal. ($C_{15}H_{19}BrN_2S$) C, H, N.

*4.1.32. 4-Benzyl-3-(4-chlorophenyl)-4H-1,2,4-triazole (**34**)*

To a solution of **33** (239.0 mg, 0.95 mmol) in MeCN (10 mL), DMF-DMA (128 μL, 0.95 mmol) was added. The reaction was heated to 50 °C for 1 h. After this time, benzylamine (101 μL, 0.85 mmol) and acetic acid (2 mL) were added and reaction was heated at 120 °C for 12 h. The solvent was removed under *vacuo*. The crude product was purified by flash chromatography on silica gel (2% MeOH in EtOAc) to give **34** (198 mg, 60%) as yellow oil. ^1H NMR (300 MHz, $CDCl_3$) δ 8.19 (s, 1H), 7.46 (dd, $J = 8.5$, 2.1 Hz, 2H), 7.41–7.33 (m, 2H), 7.30–7.23 (m, 3H), 7.06–6.96 (m, 1H), 5.17 (s, 2H); MS (ESI) *m/z* 350 $[M + H]^+$.

*4.1.33. (4-Benzyl-5-(4-chlorophenyl)-4H-1,2,4-triazol-3-yl) methanol (**35**)*

A solution of **34** (100 mg, 0.29) in formaldehyde (aq. sol. 37%,

2.8 mL) was heated under reflux for 12 h. The solvent was removed under *vacuo*. The crude product was purified by flash chromatography on silica gel (2% MeOH in EtOAc) to give **35** as yellow oil. ^{1}H NMR (300 MHz, CD_3OD) δ 7.55–7.44 (m, 4H), 7.32–7.26 (m, 2H), 7.03–6.97 (m, 2H), 5.45 (s, 2H), 4.81 (d, J = 1.2 Hz, 2H). (43 mg, 50%). MS (ESI) *m/z* 300 $[M + H]^+$.

4.1.34. 4-Benzyl-3-(chloromethyl)-5-(4-chlorophenyl)-4H-1,2,4-triazole (**36a**)

To a solution of **35** (40 mg, 0.13 mmol) in dry DCM (4 mL), pyridine (12 μL, 0.14 mmol) and thionyl chloride (13 μL, 0.16 mmol) were added at 0 °C. After 3 h an aqueous solution of sodium bicarbonate was added and the organic phase was extracted with DCM, dried over sodium sulfate, filtered and evaporated *in vacuo*. The crude product was purified by flash chromatography on silica gel (2% MeOH in DCM) to give **36a** as yellow oil (20 mg, 50%). ^{1}H NMR (300 MHz, CD_3OD) δ 7.55–7.44 (m, 4H), 7.32–7.26 (m, 2H), 7.03–6.97 (m, 2H), 5.43 (s, 2H), 4.92 (s, 2H); MS (ESI) *m/z* 319 $[M + H]^+$.

4.1.35. 2-(2-Bromo-4-chlorophenyl)-5-(chloromethyl)-1,3,4-oxadiazole (**36b**)

To a solution of **33** (200 mg, 0.8 mmol) in phosphoryl chloride (2 mL), chloroacetic aid (76 mg, 0.8 mmol) was added. The reaction mixture was heated under reflux for 12 h. After this time the mixture was cooled at 0 °C, and an aqueous solution of sodium bicarbonate (2 mL) was slowly added. The organic phase was extracted with EtOAc (3 × 5 mL), dried over sodium sulfate, filtered and evaporated *in vacuo*. The crude product was purified by flash chromatography on silica gel (15% EtOAc in petroleum ether) to give **36b** as yellow oil (49 mg, 20%). ^{1}H NMR (300 MHz, CD_3OD) δ 8.04 (d, J = 8.7 Hz, 1H), 7.94–7.89 (m, 1H), 7.60 (d, J = 8.0 Hz, 1H), 4.96 (s, 2H); ^{13}C NMR (75 MHz, CD_3OD) δ 139.13, 134.11, 132.61, 131.86, 130.09, 129.56, 128.36, 122.05, 32.49. MS (ESI) *m/z* 308 $[M + H]^+$, 330 $[M + Na]^+$.

4.1.36. 1-(5-(4-Chlorophenyl)-4H-1,2,4-triazol-3-yl)-N-(piperidin-4-ylmethyl)methanamine (**37**)

To a solution of **36a** (19 mg, 0.060 mmol) in dry MeCN (1 mL), a solution of **7** (20 mg, 0.065 mmol) in dry MeCN (2 mL), potassium carbonate (134 mg, 0.97 mmol) and a catalytic amount of potassium iodide were slowly added. The reaction mixture was heated under reflux for 1 h. After this time, the solvent was removed *in vacuo*. H_2O (1 mL) and EtOAc (5 mL) were added and the organic phase was separated, dried over sodium sulfate, filtered and evaporated *in vacuo*. The crude product was purified by flash chromatography on silica gel (2% MeOH in DCM) to give 4-(4-benzyl-5-(4-chlorophenyl)-4*H*-1,2,4-triazol-3-yl)methylamino-*N*-*tert*-butoxy carbonylpiperidine as colorless oil (21 mg, 72%). ^{1}H NMR (300 MHz, CD_3OD) δ 7.55–7.44 (m, 5H), 7.34–7.26 (m, 2H), 6.98 (d, J = 8.0 Hz, 2H), 5.47 (s, 2H), 4.02 (d, J = 13.4 Hz, 2H), 3.91 (s, 2H), 2.69 (s, 2H), 2.49 (s, 2H), 1.65 (d, J = 13.5 Hz, 2H), 1.61–1.50 (m, 1H), 1.44 (s, 9H), 1.11–0.94 (m, 2H); MS (ESI) *m/z* 497 $[M + H]^+$, 535 $[M + K]^+$. To a solution of the above product (20 mg, 0.04 mmol) in DMSO (30 μL), a solution of potassium *tert*-butoxide (34 mg, 0.30 mmol) in dry THF (1 mL) was added. The reaction environment was saturated with oxygen. After 2 h an aqueous solution of ammonium chloride (0.5 mL) was added and the organic phase was extracted with EtOAc (3 × 3 mL), dried over sodium sulfate, filtered and evaporated *in vacuo*. The crude product was purified by flash chromatography on silica gel (2% MeOH in DCM) to give [5-(4-chlorophenyl)-4*H*-1,2,4-triazol-3-yl]methylamino-methyl-*N*-*tert*-butoxy-carbonyl piperidine as yellow oil (14 mg, 87%). ^{1}H NMR (300 MHz, CD_3OD) δ 7.97 (d, J = 8.2 Hz, 2H), 7.48 (d, J = 7.9 Hz, 2H), 4.07 (d, J = 13.2, 2H), 3.96 (s, 2H), 2.77 (d, J = 12.0 Hz, 2H), 2.58 (d, J = 6.0 Hz, 2H), 1.76 (d, J = 12.4 Hz, 2H), 1.44 (s, 9H), 1.31–1.21 (m, 2H), 1.15–1.04 (m, 1H). MS (ESI) *m/z* 407 $[M + H]^+$. Starting from the above compound (15 mg, 0.03 mmol) and HCl 1 N (120 μL, 0.12 mmol), the title compound was deprotected as described for the synthesis of **1**. The crude product **37** was obtained as yellow oil without further purification (11 mg, 84%). ^{1}H NMR (300 MHz, CD_3OD) δ 8.03 (d, J = 8.2 Hz, 2H), 7.63 (d, J = 8.1 Hz, 2H), 4.62 (s, 2H), 3.46 (d, J = 12.1 Hz, 2H), 3.11 (t, J = 11.8 Hz, 2H), 2.83 (brs, 2H), 2.32 (brs, 1H), 2.14 (d, J = 11.9 Hz, 2H), 1.68 (d, J = 11.1 Hz, 2H); MS (ESI) *m/z* 397 $[M + H]^+$. Anal. ($C_{15}H_{20}ClN_5$) C, H, N.

4.1.37. 1-(5-(2-Bromo-4-chlorophenyl)-1,3,4-oxadiazol-2-yl)-N-(piperidin-4-ylmethyl)methan amine (**38**)

To a solution of **36b** (12 mg, 0.06 mmol) in dry MeCN (1 mL), a solution of **7** (20 mg, 0.065 mmol) in dry MeCN (2 mL), potassium carbonate (134 mg, 0.97 mmol) and a catalytic amount of potassium iodide were slowly added. The reaction mixture was heated under reflux for 1 h. After this time, the solvent was removed *in vacuo*. H_2O (1 mL) and EtOAc (5 mL) were added and the organic phase was separated, dried over sodium sulfate, filtered and evaporated *in vacuo*. The crude product was purified by flash chromatography on silica gel (2% MeOH in DCM) to give (5-(2-bromo-4-chlorophenyl)-1,3,4-oxadiazol-2-yl)methylaminomethyl-*N*-*tert*-butoxy carbonylpiperidine as yellow oil (25 mg, 81%). ^{1}H NMR (300 MHz, CD_3OD) δ 8.02 (d, J = 8.6 Hz, 1H), 7.89 (d, J = 5.0 Hz, 1H), 7.59 (dd, J = 8.5, 1.9 Hz, 1H), 4.08 (d, J = 5.8 Hz, 2H), 4.03 (s, 2H), 2.74 (s, 2H), 2.57 (s, 2H), 1.74 (d, J = 13.9 Hz, 2H), 1.69–1.61 (m, 1H), 1,44 (s, 9H) 1.17–0.99 (m, 2H); MS (ESI) *m/z* 508 $[M + H]^+$. Starting from the above compound (20 mg, 0.04 mmol) and HCl 1 N (160 μL, 0.16 mmol), the title compound was prepared following the procedure reported for compound **37**. The solvent was removed *in vacuo*. A saturated solution of sodium bicarbonate (1 mL) was added and the organic phase was extracted with EtOAc (3 × 3 mL), dried over sodium sulfate, filtered and evaporated *in vacuo*. The crude product was purified by flash chromatography on silica gel (10% MeOH, 1% NH_4OH, in DCM) to give **38** as yellow oil (13 mg, 82%). ^{1}H NMR (300 MHz, CD_3OD) δ 8.03 (d, J = 8.3 Hz, 1H), 7.91 (d, J = 4.9, 1H), 7.59 (d, J = 8.5 Hz, 1H), 5.48 (s, 2H), 3.39 (d, J = 12.5 Hz, 2H), 3.32–3.27 (m, 2H), 2.97 (t, J = 12.4 Hz, 2H), 2.07–1.98 (m, 2H), 1.90–1.82 (m, 1H), 1.50–1.24 (m, 2H); MS (ESI) *m/z* 386 $[M + H]^+$. Anal. for ($C_{15}H_{18}BrClN_4O$) C, H, N.

4.1.38. 2-Methyl-6-(4-(trifluoromethyl)phenyl)pyridine (**41**)

Triphenylphosphine (366 mg, 1.4 mmol) and palladium (II) acetate (20 mg, 0.1 mmol) were dissolved in a mixture of dry DMF (7 mL) and H_2O (3 mL) under argon atmosphere. After 30 min, **39** (198 μL, 1.7 mmol) was added. After further 30 min, potassium carbonate (721 mg, 5.2 mmol) and powered 4-trifluoromethylphenyl boronic acid **40** (331 mg, 1.7 mmol) were added in this order. The reaction mixture was heated at reflux for 12 h. The solvent was removed under *vacuo*. H_2O (2 mL) and EtOAc (8 mL) were added, the organic phase was separated, dried over sodium sulfate, filtered and evaporated *in vacuo*. The crude product was purified by flash chromatography on silica gel (2% EtOAc in petroleum ether) to give **41** as white solid (336 mg, 81%). ^{1}H NMR (300 MHz, $CDCl_3$) δ 8.13–8.01 (d, J = 7,83 Hz, 2H), 7.67 (d, J = 8.6 Hz, 2H), 7.56 (t, J = 7.73 Hz, 1H), 7.44 (d, J = 8.0 Hz, 1H), 7.07 (d, J = 7.8 Hz, 1H), 2.61 (s, 3H). MS (ESI) *m/z* 238 $[M + H]^+$.

4.1.39. 2-(Bromomethyl)-6-(4-trifluoromethyl)phenylpyridine (**42**)

To a solution of **41** (336 mg, 1.4 mmol) in CCl_4 (14 mL), NBS (904 mg, 5.1 mmol) and AIBN (98 mg, 0.6 mmol) were added portion wise. The reaction was heated under reflux for 12 h. The mixture was filtered on paper and the filtrate was concentrated under *vacuo*. The crude product was purified by flash

chromatography on silica gel (20% DCM in petroleum ether) to give **42** as white solid (132 mg, 30%). ^{1}H NMR (300 MHz, $CDCl_3$) δ 8.13 (d, J = 8.00 Hz, 2H), 7.81 (t, J = 7.8 Hz, 1H), 7.73 (d, J = 8.12 Hz, 2H), 7.68 (d, J = 8.0 Hz, 1H), 7.46 (d, J = 7.6 Hz, 1H), 4.63 (s, 2H); MS (ESI) *m/z* 317 $[M + H]^+$.

4.1.40. 1-(Piperidin-4-yl)-N-((6-(4-(trifluoromethyl)phenyl) pyridin-2-yl)methyl)methanamine (**43**)

To a solution of **7** (66 mg, 0.3 mmol) in dry MeCN (1 mL), was slowly added a solution of **42** (49 mg, 0.2 mmol) in dry MeCN (3 mL) and powered potassium carbonate (171 mg, 1.2 mmol). After 12 h, the solvent was removed *in vacuo*. H_2O (1 mL) and EtOAc (5 mL) were added and the organic phase was washed with an aqueous solution NaOH (1 N, 2 mL) dried over sodium sulfate, filtered and evaporated *in vacuo*. The crude product was purified by flash chromatography on silica gel (2% MeOH in DCM) to give the alkylation product 6-[4-(trifluoromethyl)phenyl-pyridin-2-yl] methylamino-methyl-*N*-*tert*-butoxycarbonyl piperidine as colorless oil. (18 mg, 20%). ^{1}H NMR: (300 MHz, CD_3OD) δ 8.25 (d, J = 8.1 Hz, 2H), 7.87–7.82 (m, 2H), 7.78 (d, J = 8.1 Hz, 2H), 7.40 (d, J = 7.0 Hz, 1H), 4.06 (d, J = 13.5 Hz, 2H), 3.99 (s, 2H), 2.76 (t, J = 12.7 Hz, 2H), 2.60 (d, J = 6.2 Hz, 2H), 1.78 (d, J = 12.0 Hz, 2H), 1.44 (s, 9H), 1.28 (s, 1H), 1.17–1.04 (m, 2H); MS (ESI) *m/z* 450 $[M + H]^+$, 472 $[M + Na]^+$. Starting from the above alkylation product (30 mg, 0.06 mmol) and HCl 1 N (240 μL, 0.24 mmol), the title compound was prepared following the deprotection procedure reported for compound **1**. The crude product was purified by flash chromatography on silica gel (10% MeOH, 1% NH_4OH, in DCM) to give **43** as yellow oil (20 mg, 98%). ^{1}H NMR (300 MHz, CD_3OD) δ 8.25 (d, J = 8.2 Hz, 2H), 7.87 (d, J = 7.3 Hz, 2H), 7.78 (d, J = 8.2 Hz, 2H), 7.40 (d, J = 7.1 Hz, 1H), 3.96 (s, 2H), 3.21 (d, J = 12.4 Hz, 2H), 2.78 (t, J = 11.4 Hz, 2H), 2.58 (d, J = 6.6 Hz, 2H), 1.91 (d, J = 13.4 Hz, 2H), 1.80 (brs, 1H), 1.27 (m, 2H); ^{13}C NMR (75 MHz, CD_3OD) δ 162.1, 159.1, 155.3, 149.1, 143.0, 138.0, 130.8, 130.4, 127.4, 126.3, 125.5, 125.4, 119.5, 54.7, 54.1, 44.7, 35.0, 29.5, 29.0, 21.8, 17.6, 13.2, 7.1, −9.3. MS (ESI) *m/z* 350 $[M + H]^+$. Anal. f ($C_{19}H_{22}F_3N_3$) C, H, N.

4.1.41. N′-[(5-(4-Bromo-2-chlorophenyl)furan-2-yl)methyl]-N′,N′-dimethylpropane-1,3-diamine (**45**)

To a solution of N^1,N^1-dimethylpropane-1,3-diamine **44** (22 μL, 0.17 mmol) in dry DCM (2 mL), was added a solution of aldehyde **5a** (45 mg 0.16 mmol) in dry DCM (5 mL). After 1 h sodium triacetoxyborohydride (51 mg, 0.24 mmol) was added at 0 °C and the mixture kept at 25 °C for 12 h. After this time, sodium cyanoborohydride (20 mg, 0.32 mmol) was added and the solution was maintained at the same temperature for further 1 h. A saturated solution of sodium bicarbonate (3 mL) was added and the organic phase was extracted with DCM (3 × 5 mL), dried over sodium sulfate, filtered and evaporated *in vacuo*. The crude product was purified by flash chromatography on silica gel (10% MeOH, 1% NH_4OH, in DCM) to give **45** as yellow oil (50 mg, 85%). ^{1}H NMR (300 MHz, CD_3OD) δ 7.82 (d, J = 6.1 Hz, 1H), 7.66 (s, 1H), 7.51 (d, J = 6.5 Hz, 1H), 7.09 (d, J = 3.2 Hz, 1H), 6.43 (d, J = 3.1 Hz, 1H), 3.83 (d, J = 2.1 Hz, 2H), 2.66 (t, J = 6.1 Hz, 2H), 2.43–2.36 (m, 2H), 2.26 (s, 6H), 1.74–1.70 (m, 2H); ^{13}C NMR (75 MHz, CD_3OD) δ 153.7, 148.7, 132.9, 130.3, 130.3, 128.8, 128.4, 120.4, 112.2, 109.8, 57.4, 46.9, 45.2, 44.1, 25.6; MS (ESI) *m/z* 394 $[M + Na]^+$. Anal. ($C_{16}H_{20}BrClN_2O$) C, H, N.

4.1.42. tert-Butyl [(5-(4-chloro-2-bromophenyl)furan-2-yl-methyl]-3-dimethylaminopropyl carbamate (**46**)

Starting from **44** (65 μL, 0.5 mmol) and **18b** (130 mg, 0.5 mmol), the title compound was prepared following the procedure reported for compound **45**. The crude product was purified by flash chromatography on silica gel (10% MeOH, 1% NH_4OH, in DCM) to give N^1-[(5-(4-chloro-2-bromophenyl)furan-2-yl-methyl]-N^3,N^3-dimethylpropane-1,3-diamine as yellow oil (92 mg, 50%). ^{1}H NMR (300 MHz, CD_3OD) δ 7.80 (d, J = 8.6 Hz, 1H), 7.68 (s, 1H), 7.43 (d, J = 9.0 Hz, 1H), 7.12 (d, J = 3.4 Hz, 1H), 6.41 (d, J = 3.4 Hz, 1H), 3.87 (s, 2H), 2.64 (t, J = 7.3 Hz, 2H), 2.41–2.26 (m, 2H), 2.22 (s, 6H), 1.80 (t J = 6.0 Hz, 2H); ^{13}C NMR (75 MHz, CD_3OD) δ 153.7, 148.7, 132.9, 130.3, 130.3, 128.8, 128.4, 120.4, 112.2, 109.8, 57.4, 46.86, 45.2, 44.1, 25.6; MS (ESI) *m/z* 394 $[M + Na]^+$. To a solution of the above secondary amine (57 mg, 0.2 mmol) in dry MeOH (4 mL), triethylamine (63 μL, 0.5 mmol) and di-*tert*-butyl dicarbonate (49 mg, 0.2 mmol) were added. The reaction mixture was kept at 25 °C for 4 h. After this time, the solvent was removed *in vacuo*. H_2O (2 mL) was added and the organic phase was extracted with EtOAc (3 × 3 mL), dried over sodium sulfate, filtered and evaporated *in vacuo*. The crude product was purified by flash chromatography on silica gel (5% MeOH in DCM) to give **46** as yellow oil (82 mg, 87%). ^{1}H NMR (400 MHz, $CDCl_3$) δ 7.65 (d, J = 8.5 Hz, 1H), 7.60 (s, 1H), 7.27 (d, J = 8.5,1H), 7.06 (s, 1H), 6,28 (br s, 1H), 4.42 (br s, 2H), 3.29 (br s, 2H), 2.19 (s, 6H), 1.67 (brs, 4H), 1.44 (s, 9H); MS (ESI) *m/z* 394 $[M + H]^+$.

4.1.43. 3-[(5-(4-Chloro-2-bromophenyl)furan-2-yl-methyl)amino]-N,N,N-trimethylpropan-1-ammonium chloride (**47**)

To a solution of **46** (30 mg, 0.1 mmol) in dry acetone (2 mL), iodomethane (16 μL, 0.3 mmol) was added. Reaction refluxed for 72 h. The solvent was removed under *vacuo*. The crude product was purified by flash chromatography on alumina gel (33% MeCN in DCM) to give (5-(2-bromo-4-chlorophenyl)furan-2-yl)methyl) (*tert*-butoxycarbonyl)amino)-*N*,*N*,*N*-trimethylpropan-1-ammonium iodide as yellow oil (29 mg, 60%). ^{1}H NMR (300 MHz, CD_3OD) δ 7.78–7.72 (m, 2H), 7.44 (d, J = 8.6 Hz, 1H), 7.12 (d, J = 3.4 Hz, 1H), 6.49 (d, J = 3.4 Hz, 1H), 4.54 (s, 2H), 3.43 (t, J = 6.9 Hz, 2H), 3.30 (s, 2H), 3.10 (s, 9H), 2.03 (br s, 2H), 1.50 (s, 9H). MS (ESI) *m/z* 485 $[M + H]^+$. To a solution of the above compound (10 mg, 0.02 mmol) in MeOH (2 mL), a solution of HCl 1 N (110 μL), prepared using acetyl chloride (355 μL, 4.97 mmol) in MeOH (4.64 mL) was added at 0 °C. The reaction mixture was kept at 25 °C for 4 h. The solvent was removed under *vacuo* to give the **47** as colorless oil without further purification (7 mg, 95%). ^{1}H NMR (300 MHz, CD_3OD) δ 7.89 (d, J = 7,01 1H), 7.48 (s, 1H), 7.21 (d, J = 3.4 Hz, 1H), 6.85 (d, J = 3.4 Hz, 1H), 4.46 (s, 2H), 3.53 (br s, 4H), 3.20 (s, 9H), 2.28 (br s, 2H). (ESI) *m/z* 385 $[M + H]^+$. Anal. for ($C_{17}H_{23}BrCl_2N_2O$) C, H, N.

4.1.44. N-Benzyl-3-[(5-(4-chloro-2-bromophenyl)furan-2-yl-methyl)amino]-N,N-dimethylpropan-1-ammonium chloride (**48**)

To a solution of **46** (30 mg, 0.1 mmol) in dry acetone (2 mL), benzyl bromide (38 μL, 0.3 mmol) was added. The reaction mixture was heated under reflux for 72 h. The solvent was removed under *vacuo*. The crude product was purified by flash chromatography on silica gel (5% MeOH in DCM) to give the benzyldimethylammonium bromide salt as yellow oil (32 mg, 58%). ^{1}H NMR (300 MHz, CD_3OD) δ 7.80–7.62 (m, 2H), 7.57–7.45 (m, 5H), 7.41 (d, J = 8.5 Hz, 1H), 7.09 (d, J = 3.5 Hz, 1H), 6.47 (d, J = 3.3 Hz, 1H), 4.54 (s, 2H), 4.49 (s, 2H), 3.46 (t, J = 6.7 Hz, 1H), 3.38–3.21 (m, 2H), 3.00 (s, 6H), 2.14 (t, J = 9.0 Hz, 2H), 1.49 (s, 9H); MS (ESI) *m/z* 562 $[M + H]^+$. To a solution of the above compound (21 mg, 0.04 mmol) in MeOH (2 mL), a solution of HCl 1 N (222 μL), prepared using acetyl chloride (355 μL, 4.97 mmol) in MeOH (4.64 mL) was added at 0 °C. The reaction mixture was kept at 25 °C for 4 h. The solvent was removed under *vacuo* to give **48** as yellow oil without further purification (17 mg, 94%). ^{1}H NMR (300 MHz, CD_3OD) δ 7.90 (d, J = 7.7 Hz, 1H), 7.73 (s, 1H), 7.65–7.42 (m, 6H), 7,20 (s, 1H), 6.85 (s, 1H), 4.60 (s, 2H), 4.45 (s, 2H), 3.51 (br s, 2H), 3.22 (br s, 2H), 3.09 (s, 6H), 2.39 (br s, 2H); MS (ESI) *m/z* 462 $[M + H]^+$. Anal. ($C_{23}H_{27}BrCl_2N_2O$) C, H, N.

4.2. Pan-assay interference compounds

Reference (**1**) and synthesized compounds were investigated for their potential capability to behave as pan-assay interference compounds (PAINS) by means of FAFDrugs4.0 [55,56]. Remarkably, none of compounds contain sub-structural features that would label them as "frequent hitters" in high throughput screens.

4.3. Antiplasmodial and gametocytocidal activity evaluation

4.3.1. Parasite growth of D10 and W2 strains

The CQ sensitive (D10) and the CQ resistant (W2) strains of *P. falciparum* were maintained *in vitro* at 5% haematocrit (human type A-positive red blood cells) in RPMI 1640 (EuroClone, Celbio) medium with the addition of 1% AlbuMax (Invitrogen, Milan, Italy), 0.01% hypoxanthine, 20 mM HEPES, and 2 mM glutamine, at 37 °C in a standard gas mixture consisting of 1% O_2, 5%CO_2, and 94% N_2 [39].

4.3.2. Antiplasmodial activity against D10 and W2 strains

Compounds were dissolved in DMSO and then diluted with medium to achieve the required concentrations (final DMSO concentration <1%, which is nontoxic to the parasite). Drugs were placed in 96 well flat-bottom microplates (COSTAR) and serial dilutions made. Asynchronous cultures with parasitemia of 1–1.5% and 1% final haematocrit were aliquoted into the plates and incubated for 72 h at 37 °C. Parasite growth was determined spectrophotometrically (OD_{650}) by measuring the activity of the parasite lactate dehydrogenase (pLDH), according to a modified version of Makler's method in control and drug-treated cultures [39]. Antiplasmodial activity is expressed as the 50%inhibitory concentrations (IC_{50}). Each IC_{50} value is the mean ± standard deviation of at least three separate experiments performed in duplicate.

4.3.3. Gametocytocidal activity against P. falciparum 3D7 strain 3D7elo1-pfs16-CBG99

Gametocytes were obtained from the transgenic *P. falciparum* 3D7 strain 3D7elo1-pfs16-CBG99 expressing the *Pyrophorus plagiophthalamus* CBG99 luciferase under the gametocyte specific promoter *pfs16*. Late-stage gametocytes (stage IV-V, evaluated by Giemsa staining) were exposed to compounds at day 8–10 after *N*-acetylglucosamine (NAG) addition. For drug susceptibility assay, compounds were prepared by serial dilution, in 96-well plate, in complete medium. Epoxomicin or methylene blue were used as reference drugs. After 72 h incubation, drug-treated gametocyte samples at 2% haematocrit were transferred to 96-well black microplates and D-luciferin (1 mM in citrate buffer 0.1 M, pH 5.5) was added at a 1:1 vol ratio. After 10 min incubation, gametocytes viability was measured as luciferase activity using a Sinergy 4 (Biotek) microplate reader (500 ms integration time). The IC_{50} was extrapolated from the non-linear regression analysis of the concentration–response curve [23].

4.3.4. NF54

Asexual blood stage parasites were seeded at a density of 0.83% in 1.5% haematocrit in RPMI1640 medium with 10% human serum and combined with compounds serially diluted in DMSO and RPMI1640 medium to reach a final DMSO concentration of 0.1% in a volume of 60 μL. Following a 72 h incubation at 37 °C, 3% O_2, 4% CO_2, 30 μL of diluted Sybrgeen reagent was added according to the instructions of the manufacturer (Life Technologies) and fluorescence intensity was quantified using a Biotek Synergy 2 plate reader.

4.3.5. NF54 gametocytes

Gametocytes were obtained from a culture flask inoculated with 1% asexual blood stage parasites in 5% haematocrit in RPMI1640 medium with 10% human serum. From day 4 to day 9 post-inoculation, cultures were treated with 50 mM NAG to eliminate asexual blood stage parasites. At day 11 post inoculation, gametocytes (predominantly stage IV) were isolated by Percoll density gradient centrifugation as described previously (PMID 25667405). Gametocytes were seeded at a density of 5000 cells/well in a 384 well plate and combined with compound diluted in DMSO and subsequently in RPMI1640 medium to reach a final DMSO concentration of 0.1% in a volume of 60 μL RPMI1640 medium with 10% human serum. Following a 72 h incubation at 37 °C, 3% O_2, 4% CO_2, 30 μL of ONE-Glo reagent (Promega) was added and luminescence was quantified using a Biotek Synergy 2 reader.

4.4. Liver-stage analysis

20'000 mCherry expressing *P. berghei* (ANKA strain) sporozoites ($PbmCherry_{hsp70}$, [57]) were used to infect mouse primary hepatocytes grown on 96-well plate (isolated as published in Prado et al. [58]). 2 hpi the cells were exposed to different concentrations of **25**, as control DMSO (equal to the highest concentration of **25**) was used. Medium/Drug was renewed at 24 hpi. At 48 hpi parasite number and size of unfixed cells were determined by automated microscopy (INcell Analyzer, 2000, Gelifesciences). At 65 hpi detached cells (DC) were transferred to new wells and counted by fluorescent microscopy (Leica DMI 6000B). The detached cell assay is presented as detached cell formation rate (DC number in % of 48 h number). Statistical analysis was done by performing One-way ANOVA with Dunnet's Multiple Comparisons (Prism, GraphPad) ($^{*}p < 0.05$, $^{**}p < 0.01$, $^{***}p < 0.001$, ns/not significant > 0.05).

4.5. Isolated rat heart experiments

4.5.1. Animals

All animal care and experimental protocols conformed to the European Union Guidelines for the Care and the Use of Laboratory Animals (European Union Directive, 2010/63/EU) and were approved by the Italian Department of Health (666/2015-PR). Male Wistar rats (300–350 g, Charles River Italia, Calco, Italy) were anaesthetized (i.p.) with a mixture of Zoletil® 100 (7.5 mg/kg tiletamine HCl + 7.5 mg/kg zolazepam HCl; Virbac srl, Milano) e Rompun® (4 mg/kg xylazine HCl; Bio 98, San Lazzaro, Bologna), containing heparin (5000 U/kg), decapitated and exsanguinated.

4.5.2. Isolated rat heart preparation and perfusion

The hearts, spontaneously beating, were rapidly explanted and mounted on a Langendorff apparatus for retrograde perfusion via the aorta at a constant flow rate of 10 mL/min with a Krebs–Henseleit solution of the following composition (mM): NaCl 118, KCl 4.7, $CaCl_2$ 2.5, $MgSO_4$ 1.2, $NaHCO_3$ 25, KH_2PO_4 1.2, glucose 11.5, Na pyruvate 2, and EDTA 0.5, bubbled with a 95% O_2–5% CO_2 gas mixture (pH 7.4), and kept at 37 °C, as described elsewhere [59]. The hearts were allowed to equilibrate for at least 20 min before drug exposure. Heart contractility was measured as LVP by means of latex balloon, inserted into the left ventricle via the mitral valve and connected to a pressure transducer (BLPR, WPI, Berlin, Germany). The balloon was inflated with deionized water from a microsyringe until a left ventricular end diastolic pressure of 10 mmHg was obtained. Alteration in CPP, arising from changes in coronary vascular resistance, were recorded by pressure transducer (BLPR, WPI, Berlin, Germany) placed in the inflow line. A surface ECG was recorded at a sampling rate of 1 kHz by means of two steel electrodes, one placed on the apex and the other on the left atrium of the heart. The ECG analysis included the following measurements: RR (cycle length), HR (frequency), PQ (atrioventricular

conduction time), QRS (intraventricular conduction time), and QT (overall action potential duration) [60]. LVP, CPP, and ECG were recorded with a digital PowerLab data acquisition system (PowerLab 8/30; ADInstruments, Castle Hill, Australia) and analyzed by using Chart Pro for Windows software (PowerLab; ADInstruments, Castle Hill, Australia). LVP was calculated by subtracting the left ventricular diastolic pressure from the left ventricular systolic pressure. As the QT interval is affected by heart rate changes (e.g., it shortens when heart rate increases), Bazett's formula normalized to average rat RR (corrected QT, $QTc = QT/(RR/f)1/2$) [61] was routinely used to correct it, in order to avoid confounding effects. In our experiments, "f", the normalization factor according to the basal RR duration was 242.23 ms for compound **1** and 217.15 ms for compound **25**, as it was the average cardiac cycle length. Analysis of data was accomplished using GraphPad Prism version 5.04 (GraphPad Software, San Diego, USA). Statistical analyses and significance as measured by repeated measures ANOVA (followed by Dunnett's post test) were obtained using GraphPad InStat version 3.06 (GraphPad Software, San Diego, USA). In all comparisons, $P < 0.05$ was considered significant. Compounds **1** and **25** were dissolved in DMSO. Solvent failed to alter the response of the preparations (data not shown).

4.6. Electrophysiological experiments

4.6.1. Cell isolation procedure and whole-cell patch-clamp recording

Rat tail was cut immediately, cleaned of skin and placed in physiological solution (namely external solution). The tail main artery was dissected free of its connective tissue and cells or rings prepared as detailed below. Smooth muscle cells were freshly isolated from the tail main artery under the following conditions: a 5-mm long piece of artery was incubated at 37 °C for 40–45 min in 2 mL of 0.1 mM Ca^{2+} external solution (in mM: 130 NaCl, 5.6 KCl, 10 Hepes, 20 glucose, 1.2 $MgCl_2$, and 5 Na-pyruvate; pH 7.4) containing 20 mM taurine (prepared by replacing NaCl with equimolar taurine), 1.35 mg/mL collagenase (type XI), 1 mg/mL soybean trypsin inhibitor, and 1 mg/mL bovine serum albumin (Sigma Chimica, Milan, Italy), which was gently bubbled with a 95% O_2 − 5% CO_2 gas mixture to gently stir the enzyme solution, as previously described [62]. Cells, stored in 0.05 mM Ca^{2+} external solution containing 20 mM taurine and 0.5 mg/mL bovine serum albumin at 4 °C under normal atmosphere, were used for experiments within two days after isolation [63]. Cells were continuously superfused with external solution containing 0.1 mM Ca^{2+} and 30 mM tetraethylammonium (TEA, Sigma Chimica, Milan, Italy) using a peristaltic pump (LKB 2132, Bromma, Sweden), at a flow rate of 400 μL/min. The conventional whole-cell patch-clamp method was employed to voltage-clamp smooth muscle cells. Recording electrodes were pulled from borosilicate glass capillaries (WPI, Berlin, Germany) and fire-polished to obtain a pipette resistance of 2–5 MΩ when filled with internal solution. The internal solution (pCa 8.4) consisted of (in mM): 100 CsCl, 10 HEPES, 11 EGTA, 2 $MgCl_2$, 1 $CaCl_2$, 5 Na-pyruvate, 5 succinic acid, 5 oxaloacetic acid, 3 Na_2-ATP and 5 phosphocreatine; pH was adjusted to 7.4 with CsOH. An Axopatch 200B patch-clamp amplifier (Molecular Devices Corporation, Sunnyvale, USA) was used to generate and apply voltage pulses to the clamped cells and record the corresponding membrane currents. At the beginning of each experiment, the junction potential between the pipette and bath solution was electronically adjusted to zero. Current signals, after compensation for whole-cell capacitance and series resistance (between 70% and 75%), were low-pass filtered at 1 kHz and digitized at 3 kHz prior to being stored on the computer hard disk. Electrophysiological responses were tested at room temperature (20–22 °C). The current through $Ca_v1.2$ channels was recorded in external solution containing 30 mM TEA and 5 mM Ba^{2+}. Current was elicited with 250-ms clamp pulses (0.067 Hz) to 0 mV from a V_h of −50 mV. Data were collected once the current amplitude had been stabilized (usually 7–10 min after the whole-cell configuration had been obtained). Under these conditions, the current did not run down during the following 40 min [64]. K^+ currents were blocked with 30 mM TEA in the external solution and Cs^+ in the internal solution. Current values were corrected for leakage and residual outward currents using 10 μM nifedipine (Sigma Chimica, Milan, Italy), which completely blocked $I_{Ca1.2}$. The osmolarity of the 30 mM TEA- and 5 mM Ba^{2+}-containing external solution (320 mosmol) and that of the internal solution (290 mosmol) were measured with an osmometer (Osmostat OM 6020, Menarini Diagnostics, Florence, Italy). Acquisition and analysis of data were accomplished using pClamp 9.2.1.9 software (Molecular Devices Corporation, Sunnyvale, USA) and GraphPad Prism version 5.04 (GraphPad Software, San Diego, USA). Compounds **1** and **25** were dissolved in DMSO (below 0.01). Solvent failed to alter the response of the preparations (data not shown).

4.7. Enzyme assays and IC_{50} analysis

For biochemical analysis of compounds, *Pf*PMT was expressed in and purified from *E. coli*, as previously described [53]. Methyltransferase activity was monitored using a radiochemical assay [52]. Standard reaction conditions were 0.1 M Hepes KOH (pH 8.0), 2 mM Na_2EDTA, 10% (v/v) glycerol, 5% (v/v) DMSO, 30 μM SAM (100 nCi of [*methyl*-^{14}C] SAM), and 55 μM phosphoethanolamine in 100 μL with 2 μg of purified protein. Initial screening of compounds **1**, **24, 25** and **48** as potential *Pf*PMT inhibitors was performed at 100 μM. For determination of the IC_{50} for compound **25** versus *Pf*PMT, assays were performed with varied inhibitor concentration (0–250 μM; final 5% (v/v) DMSO) with 100% activity defined as the control reaction (conditions as above)). Data were plotted as percentage of activity versus inhibitor concentration and were fit to $y = 100/(1 + ([I]/IC_{50}))$ using Kaleidagraph (Synergy Software), where IC_{50} is the inhibitor concentration at 50% activity.

4.8. Computational details

All calculations in this work were performed on a system comprising 72 Intel Xeon E5-2695 v4@2.10 GHz processors and two NVIDIA GeForce 1070 GTX GPU with Ubuntu 16.04 LTS (long-term support) operating system, running Schrödinger Molecular Modelling Environment Release 2015. Among the software in the molecular modelling suite we used Maestro, version 10.1; MacroModel, version 10.7; LigPrep, version 3.3; SiteMap version 3.4; Glide, version 6.6; Prime version 4.1 and PyMOL v1.8.4.0.

4.8.1. Protein and ligands preparation

We retrieved from the PDB database all proteins relevant for the *Plasmodium* biology for a total of 108 crystal structures. All the crystal structures were analyzed, removing the water molecules, ions not involved in the enzymatic reactions and molecules used for the crystallization process. For the proteins with the co-crystallized ligands (inhibitors, substrates etc) we extracted them for a re-docking procedure to assess the reliability of the docking protocol (see next paragraph for further details). The selected crystal structures were prepared by means of Protein Preparation Wizard (PPW) protocol implemented in Maestro, for acquiring appropriate starting complexes for the subsequent computational analyses. In particular, the protocol includes three steps to: (1) add hydrogens, (2) optimize the orientation of hydroxyl groups, Asn, and Gln, and the protonation state of His, and (3) perform a constrained

refinement by employing *impref* software (max RMSD = 0.30), consisting of a cycles of energy minimization based on the impact molecular mechanics engine employing OPLS_2005 as force field. Regarding *Pf*PMT, the crystal structure with the code 3UJ8 from PDB containing the inhibitor sinefungin (adenosyl-ornithine) was selected. For the redocking procedure we consider also the natural substrate SAM extracted from the *Pf*PMT crystal structure 3UJ6. Compounds **1** and **25** as well as all the ligands in the Plasmodium proteins (Sinefungin and SAM in the case of *Pf*PMT) were treated by means of MacroModel for retrieving the lower energy conformers to use as input in molecular docking experiments. The calculation was performed using OPLS-2005 as force field. The Generalized-Born/Surface-Area (GB/SA) model for simulating the solvent effects was used. No cutoff for non-bonded interactions was used. PRCG method was employed with 1000 maximum iterations and 0.001 gradient convergence threshold for performing the molecular energy minimizations. MCMM (Monte Carlo Multiple Minimum) was employed as torsional sampling method for the conformational searches, performing automatic setup with 21 kJ/mol (5.02 Kcal/mol) in the energy window for saving structure and 0.5 Å was used as cutoff distance for redundant conformers. The lower conformers were treated by LigPrep application, generating the most plausible ionization state at cellular pH value (7.4 ± 0.2).

4.8.2. Molecular docking

Molecular Docking was carried out by Glide using the ligands and the protein prepared as above-mentioned, applying Glide extra precision (XP) method. Energy grid was prepared using default value of protein atom scaling factor (1.0 Å) within a cubic box centered on the crystallized ligands were present, while for the *Plasmodium* proteins without any ligand we selected the binding site by analysing the literature data and/or performing a SiteMap calculation to find potential binding sites. Considering *Pf*PMT, the cubic box centered on the sinefungin. After grid generation, the ligands and the crystallized inhibitor were docked into the enzymes with default parameters (no constraints were added). The number of poses entered to post-docking minimization was set to 50. Glide XP score was evaluated. The interactions of compounds with proteins were assessed using ligand-interaction diagram and a script for displaying hydrophobic interactions (*display_hydrophobic_interactions.py*) downloaded from Schrödinger website and implemented in Maestro. The RMSD between the docked poses and the co-crystallized compounds was calculated by using the script *rmsd. py* available in Maestro. We chose the Glide XP protocol since it demonstrated in this virtual screening procedure better accuracy in retrieving the binding mode of the crystallized ligands, showing lower RMSD over the Glide standard precision (SP) protocol as highlighted also for *Pf*PMT. In fact, although the docking protocols were able to correctly accommodate the considered ligands (sinefungin and SAM), the Glide XP protocol showed low RMSD between the docked poses and crystallized ligands (sinefungin Glide XP RMSD = 0.21; Glide SP RMSD = 0.66. SAM Glide XP RMSD = 0.48; Glide SP RMSD = 1.05).

4.8.3. Evaluation of ligand binding energy

The Prime/MM-GBSA method (Prime software) computes the difference between both the states, free and complex, of the ligand and the protein after energy minimization as reported [50]. The calculated absolute values are not necessarily in agreement with observed binding affinities. Nonetheless, the ranking of the ligands based on the binding energies calculations (MM/GBSA ΔG_{bind}) can agree reasonably well with ranking based on observed binding affinity, particularly in the case of congeneric series. As the MM/GBSA binding energies are approximate free energies of binding, a more negative value indicates stronger binding. The technique was used on the docked complexes (ligand-protein). For each ligand the software was employed to assess its ligand binding energy (ΔG_{bind}) exploiting the following equation:

$$\Delta G_{bind} = \Delta E_{MM} + \Delta G_{solv} + \Delta G_{sa}$$

ΔE_{MM} is the difference in the minimized energies calculated for the complex and the sum of the energies of the unbounded protein and ligand. ΔG_{solv} represents the difference in the GBSA solvation energy of the complex and the sum of these energies for the unbounded protein and ligand. ΔG_{SA} is the difference in the surface area (SA) energies for the complex and the sum of the SA energies for the unbounded protein and ligand.

4.8.4. Picture preparation

Fig. 6 was prepared by means of PyMOL (The PyMOL Molecular Graphics System, v1.8.4.0, Schrödinger LLC, New York, 2015).

Acknowledgment

Financial contribution from MIUR is acknowledged. S.G.L. and J.M.J. acknowledge support from the National Institutes of Health (AI-097119). S.G. and D.T. acknowledge support from the COST Action CM1307. This work was supported by the Global Health Program of the Bill & Melinda Gates Foundation (Grant OPP1040394 to D.T.) and by MIUR- (Project 20154JRJPP to Gi.Ca. and D.T). The authors thank MMV (Medicine for Malaria Venture) for the availability of the malaria box compounds free of charge; a special acknowledgment to Laura Galastri, Paola Verducci, and Tiziana Bianchi from AVIS Comunale Milano for providing blood samples for *P. falciparum* parasite culture.

Appendix A. Supplementary data

Supplementary data related to this article can be found at https://doi.org/10.1016/j.ejmech.2018.03.024.

References

[1] World Malaria Report, 2016. http://www.who.int/malaria/publications/world-malaria-report-2016/en/.
[2] T.N. Wells, R. Hooft van Huijsduijnen, W.C. Van Voorhis, Malaria medicines: a glass half full? Nat. Rev. Drug Discov. 14 (2015) 424–442.
[3] F.J. Gamo, L.M. Sanz, J. Vidal, C. de Cozar, E. Alvarez, J.L. Lavandera, D.E. Vanderwall, D.V. Green, V. Kumar, S. Hasan, J.R. Brown, C.E. Peishoff, L.R. Cardon, J.F. Garcia-Bustos, Thousands of chemical starting points for antimalarial lead identification, Nature 465 (2010) 305–310.
[4] M. Rottmann, C. McNamara, B.K. Yeung, M.C. Lee, B. Zou, B. Russell, P. Seitz, D.M. Plouffe, N.V. Dharia, J. Tan, S.B. Cohen, K.R. Spencer, G.E. Gonzalez-Paez, S.B. Lakshminarayana, A. Goh, R. Suwanarusk, T. Jegla, E.K. Schmitt, H.P. Beck, R. Brun, F. Nosten, L. Renia, V. Dartois, T.H. Keller, D.A. Fidock, E.A. Winzeler, T.T. Diagana, Spiroindolones, a potent compound class for the treatment of malaria, Science 329 (2010) 1175–1180.
[5] S. Nakazawa Hewitt, D.M. Dranow, B.G. Horst, J.A. Abendroth, B. Forte, I. Hallyburton, C. Jansen, B. Baragana, R. Choi, K.L. Rivas, M.A. Hulverson, M. Dumais, T.E. Edwards, D.D. Lorimer, A.H. Fairlamb, D.W. Gray, K.D. Read, A.M. Lehane, K. Kirk, P.J. Myler, A. Wernimont, C.S. Walpole, R. Stacy, L.K. Barrett, I.H. Gilbert, W.C. Van Voorhis, Biochemical and structural characterization of selective allosteric inhibitors of the plasmodium falciparum drug target, prolyl-tRNA-synthetase, ACS Infect. Dis. 3 (2016) 34–44.
[6] B. Baragana, N.R. Norcross, C. Wilson, A. Porzelle, I. Hallyburton, R. Grimaldi, M. Osuna-Cabello, S. Norval, J. Riley, L. Stojanovski, F.R. Simeons, P.G. Wyatt, M.J. Delves, S. Meister, S. Duffy, V.M. Avery, E.A. Winzeler, R.E. Sinden, S. Wittlin, J.A. Frearson, D.W. Gray, A.H. Fairlamb, D. Waterson, S.F. Campbell, P. Willis, K.D. Read, I.H. Gilbert, Discovery of a quinoline-4-carboxamide derivative with a novel mechanism of action, multistage antimalarial activity, and potent in vivo efficacy, J. Med. Chem. 59 (2016) 9672–9685.
[7] R.L. Edwards, A.R. Odom John, Muddled mechanisms: recent progress towards antimalarial target identification, F1000Res 5 (2016) 2514.
[8] K. Singh, J. Okombo, C. Brunschwig, F. Ndubi, L. Barnard, C. Wilkinson, P.M. Njogu, M. Njoroge, L. Laing, M. Machado, M. Prudencio, J. Reader, M. Botha, S. Nondaba, L.M. Birkholtz, S. Lauterbach, A. Churchyard, T.L. Coetzer, J.N. Burrows, C. Yeates, P. Denti, L. Wiesner, T.J. Egan, S. Wittlin,

K. Chibale, Antimalarial pyrido[1,2-a]benzimidazoles: lead optimization, parasite life cycle stage profile, mechanistic evaluation, killing kinetics, and in vivo oral efficacy in a mouse model, J. Med. Chem. 60 (2017) 1432–1448.
[9] C. Le Manach, T. Paquet, C. Brunschwig, M. Njoroge, Z. Han, D. Gonzalez Cabrera, S. Bashyam, R. Dhinakaran, D. Taylor, J. Reader, M. Botha, A. Churchyard, S. Lauterbach, T.L. Coetzer, L.M. Birkholtz, S. Meister, E.A. Winzeler, D. Waterson, M.J. Witty, S. Wittlin, M.B. Jimenez-Diaz, M. Santos Martinez, S. Ferrer, I. Angulo-Barturen, L.J. Street, K. Chibale, A novel pyrazolopyridine with in vivo activity in plasmodium berghei- and plasmodium falciparum-infected mouse models from structure-activity relationship studies around the core of recently identified antimalarial imidazopyridazines, J. Med. Chem. 58 (2015) 8713–8722.
[10] D. Gonzalez Cabrera, F. Douelle, C. Le Manach, Z. Han, T. Paquet, D. Taylor, M. Njoroge, N. Lawrence, L. Wiesner, D. Waterson, M.J. Witty, S. Wittlin, L.J. Street, K. Chibale, Structure-activity relationship studies of orally active antimalarial 2,4-Diamino-thienopyrimidines, J. Med. Chem. 58 (2015) 7572–7579.
[11] D. Gonzalez Cabrera, C. Le Manach, F. Douelle, Y. Younis, T.S. Feng, T. Paquet, A.T. Nchinda, L.J. Street, D. Taylor, C. de Kock, L. Wiesner, S. Duffy, K.L. White, K.M. Zabiulla, Y. Sambandan, S. Bashyam, D. Waterson, M.J. Witty, S.A. Charman, V.M. Avery, S. Wittlin, K. Chibale, 2,4-Diaminothienopyrimidines as orally active antimalarial agents, J. Med. Chem. 57 (2014) 1014–1022.
[12] C. Le Manach, D. Gonzalez Cabrera, F. Douelle, A.T. Nchinda, Y. Younis, D. Taylor, L. Wiesner, K.L. White, E. Ryan, C. March, S. Duffy, V.M. Avery, D. Waterson, M.J. Witty, S. Wittlin, S.A. Charman, L.J. Street, K. Chibale, Medicinal chemistry optimization of antiplasmodial imidazopyridazine hits from high throughput screening of a SoftFocus kinase library: part 1, J. Med. Chem. 57 (2014) 2789–2798.
[13] C. Le Manach, T. Paquet, D. Gonzalez Cabrera, Y. Younis, D. Taylor, L. Wiesner, N. Lawrence, S. Schwager, D. Waterson, M.J. Witty, S. Wittlin, L.J. Street, K. Chibale, Medicinal chemistry optimization of antiplasmodial imidazopyridazine hits from high throughput screening of a softfocus kinase library: part 2, J. Med. Chem. 57 (2014) 8839–8848.
[14] M. Pieroni, E. Azzali, N. Basilico, S. Parapini, M. Zolkiewski, C. Beato, G. Annunziato, A. Bruno, F. Vacondio, G. Costantino, Accepting the invitation to open innovation in malaria drug discovery: synthesis, biological evaluation, and investigation on the structure-activity relationships of benzo[b]thiophene-2-carboxamides as antimalarial agents, J. Med. Chem. 60 (2017) 1959–1970.
[15] J.D. Bowman, E.F. Merino, C.F. Brooks, B. Striepen, P.R. Carlier, M.B. Cassera, Antiapicoplast and gametocytocidal screening to identify the mechanisms of action of compounds within the malaria box, Antimicrob. Agents Chemother. 58 (2014) 811–819.
[16] M.J. Delves, A. Ruecker, U. Straschil, J. Lelievre, S. Marques, M.J. Lopez-Barragan, E. Herreros, R.E. Sinden, Male and female Plasmodium falciparum mature gametocytes show different responses to antimalarial drugs, Antimicrob. Agents Chemother. 57 (2013) 3268–3274.
[17] S. Duffy, V.M. Avery, Identification of inhibitors of Plasmodium falciparum gametocyte development, Malar. J. 12 (2013) 408.
[18] L. Lucantoni, S. Duffy, S.H. Adjalley, D.A. Fidock, V.M. Avery, Identification of MMV malaria box inhibitors of plasmodium falciparum early-stage gametocytes using a luciferase-based high-throughput assay, Antimicrob. Agents Chemother. 57 (2013) 6050–6062.
[19] A. Ruecker, D.K. Mathias, U. Straschil, T.S. Churcher, R.R. Dinglasan, D. Leroy, R.E. Sinden, M.J. Delves, A male and female gametocyte functional viability assay to identify biologically relevant malaria transmission-blocking drugs, Antimicrob. Agents Chemother. 58 (2014) 7292–7302.
[20] N.G. Sanders, D.J. Sullivan, G. Mlambo, G. Dimopoulos, A.K. Tripathi, Gametocytocidal screen identifies novel chemical classes with Plasmodium falciparum transmission blocking activity, PLoS One 9 (2014) e105817.
[21] D.M. Plouffe, M. Wree, A.Y. Du, S. Meister, F. Li, K. Patra, A. Lubar, S.L. Okitsu, E.L. Flannery, N. Kato, O. Tanaseichuk, E. Comer, B. Zhou, K. Kuhen, Y. Zhou, D. Leroy, S.L. Schreiber, C.A. Scherer, J. Vinetz, E.A. Winzeler, High-throughput assay and discovery of small molecules that interrupt malaria transmission, Cell Host Microbe 19 (2016) 114–126.
[22] W. Sun, T.Q. Tanaka, C.T. Magle, W. Huang, N. Southall, R. Huang, S.J. Dehdashti, J.C. McKew, K.C. Williamson, W. Zheng, Chemical signatures and new drug targets for gametocytocidal drug development, Sci. Rep. 4 (2014) 3743.
[23] S. D'Alessandro, G. Camarda, Y. Corbett, G. Siciliano, S. Parapini, L. Cevenini, E. Michelini, A. Roda, D. Leroy, D. Taramelli, P. Alano, A chemical susceptibility profile of the Plasmodium falciparum transmission stages by complementary cell-based gametocyte assays, J. Antimicrob. Chemother. 71 (2016) 1148–1158.
[24] S. D'Alessandro, F. Silvestrini, K. Dechering, Y. Corbett, S. Parapini, M. Timmerman, L. Galastri, N. Basilico, R. Sauerwein, P. Alano, D. Taramelli, A Plasmodium falciparum screening assay for anti-gametocyte drugs based on parasite lactate dehydrogenase detection, J. Antimicrob. Chemother. 68 (2013) 2048–2058.
[25] W.C. Van Voorhis, J.H. Adams, R. Adelfio, V. Ahyong, M.H. Akabas, P. Alano, A. Alday, Y. Aleman Resto, A. Alsibaee, A. Alzualde, K.T. Andrews, S.V. Avery, V.M. Avery, L. Ayong, M. Baker, S. Baker, C. Ben Mamoun, S. Bhatia, Q. Bickle, L. Bounaadja, T. Bowling, J. Bosch, L.E. Boucher, F.F. Boyom, J. Brea, M. Brennan, A. Burton, C.R. Caffrey, G. Camarda, M. Carrasquilla, D. Carter, M. Belen Cassera, K. Chih-Chien Cheng, W. Chindaudomsate, A. Chubb, B.L. Colon, D.D. Colon-Lopez, Y. Corbett, G.J. Crowther, N. Cowan, S. D'Alessandro, N. Le Dang, M. Delves, J.L. DeRisi, A.Y. Du, S. Duffy, S. Abd El-Salam El-Sayed, M.T. Ferdig, J.A. Fernandez Robledo, D.A. Fidock, I. Florent, P.V. Fokou, A. Galstian, F.J. Gamo, S. Gokool, B. Gold, T. Golub, G.M. Goldgof, R. Guha, W.A. Guiguemde, N. Gural, R.K. Guy, M.A. Hansen, K.K. Hanson, A. Hemphill, R. Hooft van Huijsduijnen, T. Horii, P. Horrocks, T.B. Hughes, C. Huston, I. Igarashi, K. Ingram-Sieber, M.A. Itoe, A. Jadhav, A. Naranuntarat Jensen, L.T. Jensen, R.H. Jiang, A. Kaiser, J. Keiser, T. Ketas, S. Kicka, S. Kim, K. Kirk, V.P. Kumar, D.E. Kyle, M.J. Lafuente, S. Landfear, N. Lee, S. Lee, A.M. Lehane, F. Li, D. Little, L. Liu, M. Llinas, M.I. Loza, A. Lubar, L. Lucantoni, I. Lucet, L. Maes, D. Mancama, N.R. Mansour, S. March, S. McGowan, I. Medina Vera, S. Meister, L. Mercer, J. Mestres, A.N. Mfopa, R.N. Misra, S. Moon, J.P. Moore, F. Morais Rodrigues da Costa, J. Muller, A. Muriana, S. Nakazawa Hewitt, B. Nare, C. Nathan, N. Narraidoo, S. Nawaratna, K.K. Ojo, D. Ortiz, G. Panic, G. Papadatos, S. Parapini, K. Patra, N. Pham, S. Prats, D.M. Plouffe, S.A. Poulsen, A. Pradhan, C. Quevedo, R.J. Quinn, C.A. Rice, M. Abdo Rizk, A. Ruecker, R. St Onge, R. Salgado Ferreira, J. Samra, N.G. Robinett, U. Schlecht, M. Schmitt, F. Silva Villela, F. Silvestrini, R. Sinden, D.A. Smith, T. Soldati, A. Spitzmuller, S.M. Stamm, D.J. Sullivan, W. Sullivan, S. Suresh, B.M. Suzuki, Y. Suzuki, S.J. Swamidass, D. Taramelli, L.R. Tchokouaha, A. Theron, D. Thomas, K.F. Tonissen, S. Townson, A.K. Tripathi, V. Trofimov, K.O. Udenze, I. Ullah, C. Vallieres, E. Vigil, J.M. Vinetz, P. Voong Vinh, H. Vu, N.A. Watanabe, K. Weatherby, P.M. White, A.F. Wilks, E.A. Winzeler, E. Wojcik, M. Wree, W. Wu, N. Yokoyama, P.H. Zollo, N. Abla, B. Blasco, J. Burrows, B. Laleu, D. Leroy, T. Spangenberg, T. Wells, P.A. Willis, Open source drug discovery with the malaria box compound collection for neglected diseases and beyond, PLoS Pathog. 12 (2016) e1005763.
[26] T. Spangenberg, J.N. Burrows, P. Kowalczyk, S. McDonald, T.N. Wells, P. Willis, The open access malaria box: a drug discovery catalyst for neglected diseases, PLoS One 8 (2013), e62906.
[27] W.A. Guiguemde, A.A. Shelat, D. Bouck, S. Duffy, G.J. Crowther, P.H. Davis, D.C. Smithson, M. Connelly, J. Clark, F. Zhu, M.B. Jimenez-Diaz, M.S. Martinez, E.B. Wilson, A.K. Tripathi, J. Gut, E.R. Sharlow, I. Bathurst, F. El Mazouni, J.W. Fowble, I. Forquer, P.L. McGinley, S. Castro, I. Angulo-Barturen, S. Ferrer, P.J. Rosenthal, J.L. Derisi, D.J. Sullivan, J.S. Lazo, D.S. Roos, M.K. Riscoe, M.A. Phillips, P.K. Rathod, W.C. Van Voorhis, V.M. Avery, R.K. Guy, Chemical genetics of Plasmodium falciparum, Nature 465 (2010) 311–315.
[28] S. Meister, D.M. Plouffe, K.L. Kuhen, G.M. Bonamy, T. Wu, S.W. Barnes, S.E. Bopp, R. Borboa, A.T. Bright, J. Che, S. Cohen, N.V. Dharia, K. Gagaring, M. Gettayacamin, P. Gordon, T. Groessl, N. Kato, M.C. Lee, C.W. McNamara, D.A. Fidock, A. Nagle, T.G. Nam, W. Richmond, J. Roland, M. Rottmann, B. Zhou, P. Froissard, R.J. Glynne, D. Mazier, J. Sattabongkot, P.G. Schultz, T. Tuntland, J.R. Walker, Y. Zhou, A. Chatterjee, T.T. Diagana, E.A. Winzeler, Imaging of Plasmodium liver stages to drive next-generation antimalarial drug discovery, Science 334 (2011) 1372–1377.
[29] S. Kotha, K. Lahiri, D. Kashinath, Recent applications of the Suzuki-Miyaura cross-coupling reaction in organic synthesis, Tetrahedron 58 (2002) 9633–9695.
[30] S. Gemma, E. Gabellieri, S. Sanna Coccone, F. Marti, O. Taglialatela-Scafati, E. Novellino, G. Campiani, S. Butini, Synthesis of dihydroplakortin, 6-epi-dihydroplakortin, and their C10-desethyl analogues, J. Org. Chem. 75 (2010) 2333–2340.
[31] G. Bartoli, E. Marcantoni, L. Sambri, The CeCl3 center dot nH(2)O/NaI system in organic synthesis: an efficient water tolerant Lewis acid promoter, Synlett (2003) 2101–2116.
[32] N.D. Obushak, A.I. Lesyuk, Y.I. Gorak, V.S. Matiichuk, Mechanism of Meerwein arylation of furan derivatives, Russ. J. Org. Chem. 45 (2009) 1375–1381.
[33] M.G. Bell, M.J. Genin, P.A. Lander, L.S. Stelzer, R.A. Doti, F.J. Agejas-Chicharro, A.B. Bueno Melendo, P.R. Manninen, J.M. Ochoada, Q. Shen, A.M. Warshawsky, T. Ma, R.E. Stites, Preparation of 3-Phenylisoxazole Derivatives for Treatment of Dyslipidemia, Eli Lilly and Company, USA, 2007.
[34] M.C. Bagley, J.E. Dwyer, M.D.B. Molina, A.W. Rand, H.L. Rand, N.C.O. Tomkinson, Microwave-assisted synthesis of 3-aminobenzo[b]-thiophene scaffolds for the preparation of kinase inhibitors, Org. Biomol. Chem. 13 (2015) 6814–6824.
[35] M.J. Stocks, D.R. Cheshire, R. Reynolds, Efficient and regiospecific one-pot synthesis of substituted 1,2,4-triazoles, Org. Lett. 6 (2004) 2969–2971.
[36] A.A. Haddach, A. Kelleman, M.V. Deaton-Rewolinski, An efficient method for the N-debenzylation of aromatic heterocycles, Tetrahedron Lett. 43 (2002) 399–402.
[37] K. Zhang, P. Wang, L.N. Xuan, X.Y. Fu, F. Jing, S. Li, Y.M. Liu, B.Q. Chen, Synthesis and antitumor activities of novel hybrid molecules containing 1,3,4-oxadiazole and 1,3,4-thiadiazole bearing Schiff base moiety, Bioorg. Med. Chem. Lett. 24 (2014) 5154–5156.
[38] S. Gemma, C. Camodeca, M. Brindisi, S. Brogi, G. Kukreja, S. Kunjir, E. Gabellieri, L. Lucantoni, A. Habluetzel, D. Taramelli, N. Basilico, R. Gualdani, F. Tadini-Buoninsegni, G. Bartolommei, M.R. Moncelli, R.E. Martin, R.L. Summers, S. Lamponi, L. Savini, I. Fiorini, M. Valoti, E. Novellino, G. Campiani, S. Butini, Mimicking the intramolecular hydrogen bond: synthesis, biological evaluation, and molecular modeling of benzoxazines and quinazolines as potential antimalarial agents, J. Med. Chem. 55 (2012) 10387–10404.
[39] S. Gemma, C. Camodeca, S. Sanna Coccone, B.P. Joshi, M. Bernetti, V. Moretti, S. Brogi, M.C. Bonache de Marcos, L. Savini, D. Taramelli, N. Basilico,

S. Parapini, M. Rottmann, R. Brun, S. Lamponi, S. Caccia, G. Guiso, R.L. Summers, R.E. Martin, S. Saponara, B. Gorelli, E. Novellino, G. Campiani, S. Butini, Optimization of 4-aminoquinoline/clotrimazole-based hybrid antimalarials: further structure-activity relationships, in vivo studies, and preliminary toxicity profiling, J. Med. Chem. 55 (2012) 6948–6967.
[40] M.W. Vos, W.J. Stone, K.M. Koolen, G.J. van Gemert, B. van Schaijk, D. Leroy, R.W. Sauerwein, T. Bousema, K.J. Dechering, A semi-automated luminescence based standard membrane feeding assay identifies novel small molecules that inhibit transmission of malaria parasites by mosquitoes, Sci. Rep. 5 (2015) 18704.
[41] N. Basilico, M. Migotto, D.P. Ilboudo, D. Taramelli, R. Stradi, E. Pini, Modified quaternary ammonium salts as potential antimalarial agents, Bioorg. Med. Chem. 23 (2015) 4681–4687.
[42] M. Brindisi, S. Butini, S. Franceschini, S. Brogi, F. Trotta, S. Ros, A. Cagnotto, M. Salmona, A. Casagni, M. Andreassi, S. Saponara, B. Gorelli, P. Weikop, J.D. Mikkelsen, J. Scheel-Kruger, K. Sandager-Nielsen, E. Novellino, G. Campiani, S. Gemma, Targeting dopamine D and serotonin 5-HT and 5-HT receptors for developing effective antipsychotics: synthesis, biological characterization, and behavioral studies, J. Med. Chem. 26 (2014) 9575–9597.
[43] E.N. Prystowsky, The effects of slow channel blockers and beta blockers on atrioventricular nodal conduction, J. Clin. Pharmacol. 28 (1988) 6–21.
[44] A. Lee, K. Lee, D. Kim, Using reverse docking for target identification and its applications for drug discovery, Expert Opin. Drug Disc. 11 (2016) 707–715.
[45] S. Butini, M. Brindisi, S. Brogi, S. Maramai, E. Guarino, A. Panico, A. Saxena, V. Chauhan, R. Colombo, L. Verga, E. De Lorenzi, M. Bartolini, V. Andrisano, E. Novellino, G. Campiani, S. Gemma, Multifunctional cholinesterase and amyloid beta fibrillization modulators. Synthesis and biological investigation, ACS Med. Chem. Lett. 4 (2013) 1178–1182.
[46] Glide. version 6.6, Schrödinger, LLC, New York, NY, 2015.
[47] L. Zaccagnini, S. Brogi, M. Brindisi, S. Gemma, G. Chemi, G. Legname, G. Campiani, S. Butini, Identification of novel fluorescent probes preventing PrPSc replication in prion diseases, Eur. J. Med. Chem. 127 (2017) 859–873.
[48] C.C. Maquiaveli, J.F. Lucon, S. Brogi, G. Campiani, S. Gemma, P.C. Vieira, E.R. Silva, Verbascoside inhibits promastigote growth and arginase activity of Leishmania amazonensis, J. Nat. Prod. 79 (2016) 1459–1463.
[49] Prime. version 3.9, Schrödinger, LLC, New York, NY, 2015.
[50] M. Brindisi, S. Gemma, S. Kunjir, L. Di Cerbo, S. Brogi, S. Parapini, S. D'Alessandro, D. Taramelli, A. Habluetzel, S. Tapanelli, S. Lamponi, E. Novellino, G. Campiani, S. Butini, Synthetic spirocyclic endoperoxides: new antimalarial scaffolds, Medchemcomm 6 (2015) 357–362.
[51] S. Giovani, M. Penzo, S. Brogi, M. Brindisi, S. Gemma, E. Novellino, M.J. Blackman, G. Campiani, S. Butini, Rational design of the first difluorostatone-based PfSUB1 inhibitors, Bioorg. Med. Chem. Lett. 24 (2014) 3582–3586.
[52] S.G. Lee, W. Haakenson, J.P. McCarter, D.J. Williams, M.C. Hresko, J.M. Jez, Thermodynamic evaluation of ligand binding in the plant-like phosphoethanolamine methyltransferases of the parasitic nematode Haemonchus contortus, J. Biol. Chem. 286 (2011) 38060–38068.
[53] S.G. Lee, Y. Kim, T.D. Alpert, A. Nagata, J.M. Jez, Structure and reaction mechanism of phosphoethanolamine methyltransferase from the malaria parasite Plasmodium falciparum: an antiparasitic drug target, J. Biol. Chem. 287 (2012) 1426–1434.
[54] G. Pessi, G. Kociubinski, C.B. Mamoun, A pathway for phosphatidylcholine biosynthesis in Plasmodium falciparum involving phosphoethanolamine methylation, Proc. Natl. Acad. Sci. U. S. A. 101 (2004) 6206–6211.
[55] FAF*Drugs*4. http://fafdrugs3.mti.univ-paris-diderot.fr.
[56] D. Lagorce, O. Sperandio, J.B. Baell, M.A. Miteva, B.O. Villoutreix, FAF-Drugs3: a web server for compound property calculation and chemical library design, Nucleic Acids Res. 43 (2015) W200–W207.
[57] P.C. Burda, M.A. Roelli, M. Schaffner, S.M. Khan, C.J. Janse, V.T. Heussler, A Plasmodium phospholipase is involved in disruption of the liver stage parasitophorous vacuole membrane, PLoS Pathog. 11 (2015) e1004760.
[58] M. Prado, N. Eickel, M. De Niz, A. Heitmann, C. Agop-Nersesian, R. Wacker, J. Schmuckli-Maurer, R. Caldelari, C.J. Janse, S.M. Khan, J. May, C.G. Meyer, V.T. Heussler, Long-term live imaging reveals cytosolic immune responses of host hepatocytes against Plasmodium infection and parasite escape mechanisms, Autophagy 11 (2015) 1561–1579.
[59] S. Saponara, A. Ferrara, B. Gorelli, A. Shah, M. Kawase, N. Motohashi, J. Molnar, G. Sgaragli, F. Fusi, 3,5-dibenzoyl-4-(3-phenoxyphenyl)-1,4-dihydro-2,6-dimethylpyridine (DP7): a new multidrug resistance inhibitor devoid of effects on Langendorff-perfused rat heart, Eur. J. Pharmacol. 563 (2007) 160–163.
[60] A. Ferrara, F. Fusi, B. Gorelli, G. Sgaragli, S. Saponara, Effects of freeze-dried red wine on cardiac function and ECG of the Langendorff-perfused rat heart, Can. J. Physiol. Pharmacol. 92 (2014) 171–174.
[61] J. Kmecova, J. Klimas, Heart rate correction of the QT duration in rats, Eur. J. Pharmacol. 641 (2010) 187–192.
[62] F. Fusi, F. Manetti, M. Durante, G. Sgaragli, S. Saponara, The vasodilator papaverine stimulates L-type Ca(2+) current in rat tail artery myocytes via a PKA-dependent mechanism, Vascul. Pharmacol. (Basel) 76 (2016) 53–61.
[63] P. Mugnai, M. Durante, G. Sgaragli, S. Saponara, G. Paliuri, S. Bova, F. Fusi, L-type Ca(2+) channel current characteristics are preserved in rat tail artery myocytes after one-day storage, Acta Physiol. 211 (2014) 334–345.
[64] F. Fusi, G. Sgaragli, M. Ha le, N.M. Cuong, S. Saponara, Mechanism of osthole inhibition of vascular Ca(v)1.2 current, Eur. J. Pharmacol. 680 (2012) 22–27.